Two neuropeptides that promote blood-feeding in *Anopheles stephensi* mosquitoes

Prashali Bansal[1], **Roshni Pillai**[1,2], **Pooja DB**[1], **and Sonia Q Sen**[1,✉]

[1]Tata Institute for Genetics and Society, UAS-GKVK Campus, Bellary Road, Bangalore, India
[2]Currently at Institute of Developmental Biology and Neurobiology, Johannes Gutenberg University, Mainz, Germany

Animals routinely need to make decisions about what to eat and when. These decisions are influenced not only by the availability and quality of food but also by the internal state of the animal, which needs to compute and give weights to these different variables before making a choice. Feeding preferences of female mosquitoes exemplify this behavioural plasticity. Both male and female mosquitoes usually feed on carbohydrate-rich sources of nectar or sap, but the female also feeds on blood, which is essential for egg development. This blood-appetite is modulated across the female's reproductive cycle, yet little is known about the factors that bring it about. We show that *Anopheles stephensi* females, a major vector of urban malaria in the Indian sub-continent and West-Africa, suppress blood-feeding between a blood-meal and oviposition. We identify several candidate genes through transcriptomics of blood- deprived and -sated *An. stephensi* midbrains that could modulate this behaviour. We show that short *Neuropeptide-F (sNPF)* and *RYamide (RYa)* act together to promote blood-feeding and identify a cluster of cells in the subesophageal ganglion that expresses *sNPF* only in the blood-hungry state. Such females also have more *sNPF* in their midguts. We propose that increased *sNPF* levels in the brain and gut promotes a state of blood-hunger, which may drive feeding behaviour either by *sNPF's* action in the two tissues independently or via a communication between them.

Anopheles stephensi **| Blood-feeding | Host-seeking | Transcriptomics |** ***sNPF*** **|** ***RYamide***

Correspondence: ***sonia.sen@tigs.res.in***

An animal's dietary choice is an outcome of its internal physiological state and external stimuli. Its changing nutritional demands, reproductive state, and developmental history are integrated with external cues before a food-choice is made. For example, when deprived of a particular nutrient, like proteins, animals show a specific increase in protein-appetite (1–3). Mating influences food choices of female flies by increasing their preference for proteins, sugars, and salt for egg development and oviposition (4–8).

Changes in both sensory perception and central brain circuits have been shown to underlie such behavioural changes. For example, sensory neurons of starved animals become more sensitive to attractive cues and less sensitive to aversive ones, both in vertebrates and invertebrates (9–16). These changes are often brought about by neuromodulators and neuropeptides (9, 10, 17–22). In the central brain, internal nutrient or hormone sensors can monitor the animal's nutritional state. In mice, neurons in the hypothalamus express receptors for hunger and satiety signals like ghrelin and leptin (16, 23, 24). In insects, several neurons in the mushroom body, central complex, and subesophageal ganglion (SOG) region have been shown to integrate hunger and satiety signals to regulate feeding on sugars or proteins, choose between exploration or exploitation of food sources, or initiate or terminate feeding (25–33).

Many female mosquitoes have a dual appetite for carbohydrate-rich nectar or sap – to meet energetic requirements – and protein-rich blood – for egg development. Consequently, the female mosquito oscillates between a state of increased blood-appetite and its suppressed state through multiple reproductive cycles (figure 1A). What molecular signals control these switches in dietary preference is of great interest not only because of its importance in public health, but also because understanding how the internal state influences dietary choice of an organism has implications in other organisms. In *Aedes albopictus* anticipatory expression of the yolk protein precursor gene *vitellogenin 2* in the fat body promotes host-seeking behaviour (34). In *Aedes aegypti*, neuropeptide-Y receptor (NPYLR7), and more recently, short Neuropeptide F (sNPF) and neuropeptide RYamide (RYa) have been shown to suppresses blood-feeding, while Neuropeptide F (NPF) promotes it (35–39). Factors from the host can also both promote (ATP) (40) and terminate feeding (Fibrinopeptide A)(41).

Here we describe the blood- and sugar-feeding patterns of *Anopheles stephensi*, which is endemic to the Indian sub-continent but has expanded its range into West Africa, putting millions more people at risk of malaria (42) . Neurotranscriptomics across the different conditions of blood-deprivation and -satiety allowed us to shortlist several candidate molecules that might promote blood-feeding behaviour. Through dsRNA mediated knockdown of nine of them, we identified two neuropeptide genes – *sNPF* and *RYa* - that together promote blood-feeding through its action in the brain and possibly the abdomen. We find that *sNPF* expression pattern reflects this requirement: a cluster of cells in the SOG expresses *sNPF* only in blood-hungry females and such females also have more *sNPF* in their midguts. *RYa* is not modulated similarly. Both their receptors are expressed in the brain and the *sNPF receptor* is also expressed in the midgut. Together, these data suggest that increase in levels of *sNPF* in the brain (released by cells in the SOG) and the midgut promotes a state of blood-hunger in *An. stephensi*.

Blood-, but not sugar-feeding, is modulated across the reproductive cycle. To assess the female *An. stephensi* appetite for blood through her reproductive cycle we designed a

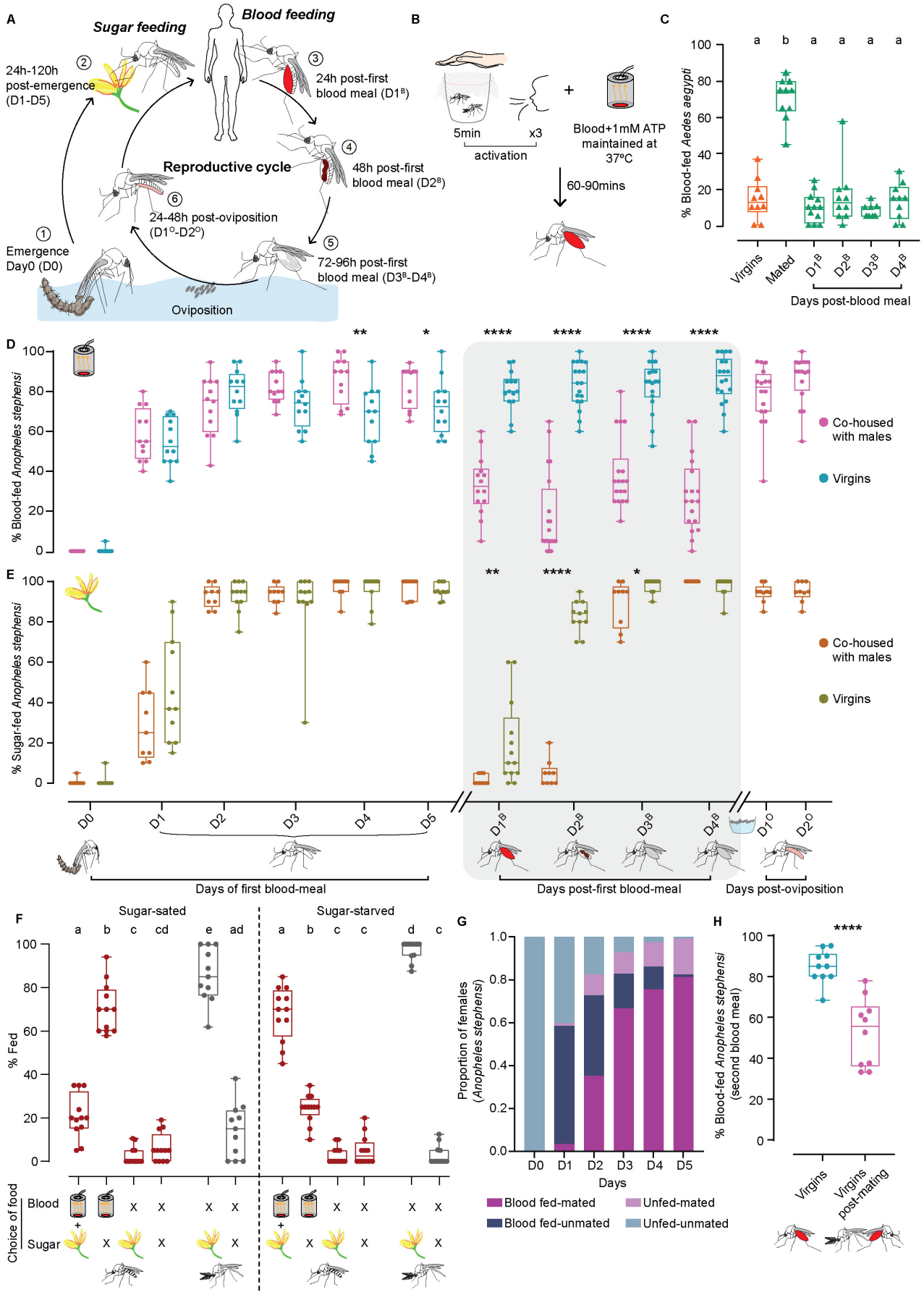
A
Sugar feeding
Blood feeding
24h-120h post-emergence (D1-D5)
24h post-first blood meal (D1B)
48h post-first blood meal (D2B)
Reproductive cycle
24-48h post-oviposition (D1O-D2O)
72-96h post-first blood meal (D3B-D4B)
Emergence Day0 (D0)
Oviposition
B
5min
x3
activation
Blood+1mM ATP maintained at 37ºC
60-90mins
C
% Blood-fed Aedes aegypti
Virgins
Mated
Days post-blood meal
D
% Blood-fed Anopheles stephensi
Co-housed with males
Virgins
E
% Sugar-fed Anopheles stephensi
Days of first blood-meal
Days post-first blood-meal
Days post-oviposition
F
Sugar-sated
Sugar-starved
% Fed
Choice of food
Blood
Sugar
G
Proportion of females (Anopheles stephensi)
Days
Blood fed-mated
Blood fed-unmated
Unfed-mated
Unfed-unmated
H
% Blood-fed Anopheles stephensi (second blood meal)
Virgins
Virgins post-mating

Fig. 1. Feeding behaviours of *An. stephensi*. A. Reproductive cycle of *An. stephensi*. Upon emergence [1, D0-D5] females have a dual appetite for protein-rich blood and carbohydrate-rich sources of sugar [2,3]. After a blood-meal [3,4,5, $D1^B$-$D4^B$], the eggs mature and are laid in water [6]. The next reproductive cycle can now begin. B. Blood-feeding assay. 0-7h old mosquitoes were collected in cups and aged appropriately on sugar. Prior to the test, mosquitoes were 'activated' for 5 minutes by presenting a human hand, followed by 3 exhalations. Blood-meals were presented through a Hemotek perfumed with human skin odours. Number of blood-fed mosquitoes were visually scored, irrespective of the quantity fed. C. Blood-feeding behaviour of *Ae. aegypti*. 8-days old virgin and mated females were assessed for their first blood-meal. Fully fed mated females were assessed for second blood-meal ($D1^B$-$D4^B$). Each dot represents a single trial with 18-21 females, n=10-12trials/group. Kruskal-Wallis, with Dunn's multiple comparisons test, $p<0.05$. Data labelled with different letters are significantly different. D. Blood-feeding behaviour of *An. stephensi*. Co-housed and virgin females were tested on the day of emergence (D0) and each day for the next 5 days (D1-D5). $D1^B$-$D4^B$ represents their blood-feeding 1-4 days after their first blood-meal and $D1^O$-$D2^O$ represents their blood-feeding 1-2 days after oviposition (see methods for assay details). 18-21females/trial, n=9-20trials/group. Two-tailed Mann-Whitney U test, $p<0.05$.*$p<0.05$, **$p<0.01$, ****$p<0.0001$. E. Sugar-feeding behaviour of *An. stephensi*. Females of similar conditions as in (D) were tested for sugar-feeding. 18-21females/trial, n=9-20trials/group. Two-tailed Mann-Whitney U test, $p<0.05$.*$p<0.05$, **$p<0.01$, ****$p<0.0001$. F. Choice assay for blood and sugar. Sugar-sated females or sugar-starved females, co-housed with males (indicated by the dashed abdomens) were given a choice between blood and sugar and assessed for their choice of food (bottom): blood and sugar; blood only; sugar only; none. While most sugar-sated females took blood (left of dashed line), most sugar-starved females fed on both (right of dashed line). As an internal control, co-housed males were accessed for sugar-feeding only and most were found to be fed in both conditions. 17-24 mosquitoes/trial; n=11-12 trials/condition. One-way Anova with Holm-Šídák multiple comparisons test, $p<0.05$. Data labelled with different letters are significantly different. G. Mating and blood-feeding. The mating status of D0-D5 co-housed females assayed in (D) were determined post-hoc by dissecting their spermathecae. n=232-239 females were analysed for each day. Many blood-fed females were unmated. H. Mating after blood-feeding. Blood-fed virgins were allowed to mate and then offered a second blood-meal. A suppression in blood-appetite was observed. 15-20females/trial, n=10 trials. Unpaired t-test, $p<0.05$.****$p<0.0001$.

behavioural assay (figure 1B, S1A; see methods for details), and tested it on *Ae. aegypti*, a well-studied model. We were able to reproduce the previously reported results that mating enhances blood-feeding in *Aedes* (43–45) and that once fed to repletion, females actively suppress blood-feeding until oviposition (46) (figure 1C).

Using this assay on *An. stephensi*, we found that these females were uninterested in blood when they emerge but that their appetite increased with age (magenta, D0-D5 in figure 1D). Once fed to repletion, like *Ae. aegypti*, *An. stephensi* also suppress blood-feeding for at least four days after a blood-meal (magenta, $D1^B$-$D4^B$ in figure 1D) and until oviposition, after which, the suppression is lifted to pre-blood-meal levels (magenta, $D1^O$-$D2^O$ in figure 1D). Unlike blood-feeding, sugar-feeding is not modulated similarly barring a brief suppression post-blood-meal, which was not dependent on oviposition (figure 1E; methods and S1G for details). Surprisingly, on the day of emergence, female mosquitoes were uninterested in both sugar- and blood-feeding (compare D0 in figure 1D, E).

To ascertain whether sugar and blood represent parallel appetites independent of each other, we presented sugar-sated co-housed females a choice between the two. Under these conditions, 70% females chose blood and only 21% took both, suggesting that the two are independent appetites (figure 1F). We next deprived co-housed females of sugars for a day before offering them the choice and found that 68% females now took both meals, while only 24% took just blood (figure 1F). As expected, males fed well on sugar in both conditions (grey, figure 1F). These data suggest that when females emerge, blood and sugar are independent appetites that exist in parallel. An interdependence of the appetites may emerge in subsequent stages of the reproductive cycle.

As mating promotes first blood-meal in *Ae. aegypti*, we tested if this was true for *An. stephensi*. A post-hoc dissection of each female's spermatheca (where sperm is stored after mating) revealed that many of the blood-fed females in the above assay were unmated (figure 1G). To confirm this, we assayed blood-feeding behaviour in virgin females and found that virgin *An. stephensi*, unlike *Ae. aegypti*, have a robust appetite for blood and that mating enhances it only marginally (cyan, D0-D5, figure 1D). Interestingly, however, these virgins, unlike mated *An. stephensi (or Ae. aegypti)* females, failed to suppress their blood-appetite, even after engorging on blood. Instead, they continued to blood-feed for up to four days after their first blood-meal (cyan, $D1^B$ - $D4^B$ in figure 1D). A flipped order of the two behaviours - virgins were first given a blood-meal then allowed to mate – also resulted in suppression of the appetite (figure 1H). This suggests that the post-blood-meal suppression of blood-appetite in *An. stephensi*, is dependent upon mating status.

Together, these data describe female *An. stephensi's* feeding behaviours: 1) in newly- emerged females blood and sugar represent parallel appetites, 2) blood-, but not sugar-appetite (barring a brief effect), is suppressed between a blood-meal and oviposition, and 3) mating is not necessary for blood-feeding in newly-emerged females, but it is necessary for its suppression between a blood-meal and oviposition.

Host-seeking is modulated across the reproductive cycle. The modulation of blood-feeding through the reproductive cycle could be due to 1) modulation in peripheral sensitivity to host kairomones, 2) modulation by central brain circuits, or 3) modulation in both peripheral and central circuit elements. Extensive data in other mosquito species suggest that sensitivity to host kairomones change as females age (47–49) and following a blood-meal (50–52). We tested this in *An. stephensi*.

Because of the multi-sensory nature of host-seeking, we used a two-choice behavioural assay where multiple host-cues were provided in one arm while the other had none. Mosquitoes had to make a choice between the two arms (figure 2A). When no host-cues are provided in either (blank) even blood-hungry females distribute equally between the two arms demonstrating the assay has no bias (black, figure 2B). Using this assay, we found that newly emerged females showed no preference for either the control or the host arm (figure 2B). Five days later, they were strongly attracted to the host-cues and this attraction was suppressed after their blood-meal and until oviposition (magenta, figure 2B). This general trend in attraction to host-cues tracks the trend in blood-feeding. Interestingly, the response of virgin females to host-cues in the Y-maze was highly variable under all con-

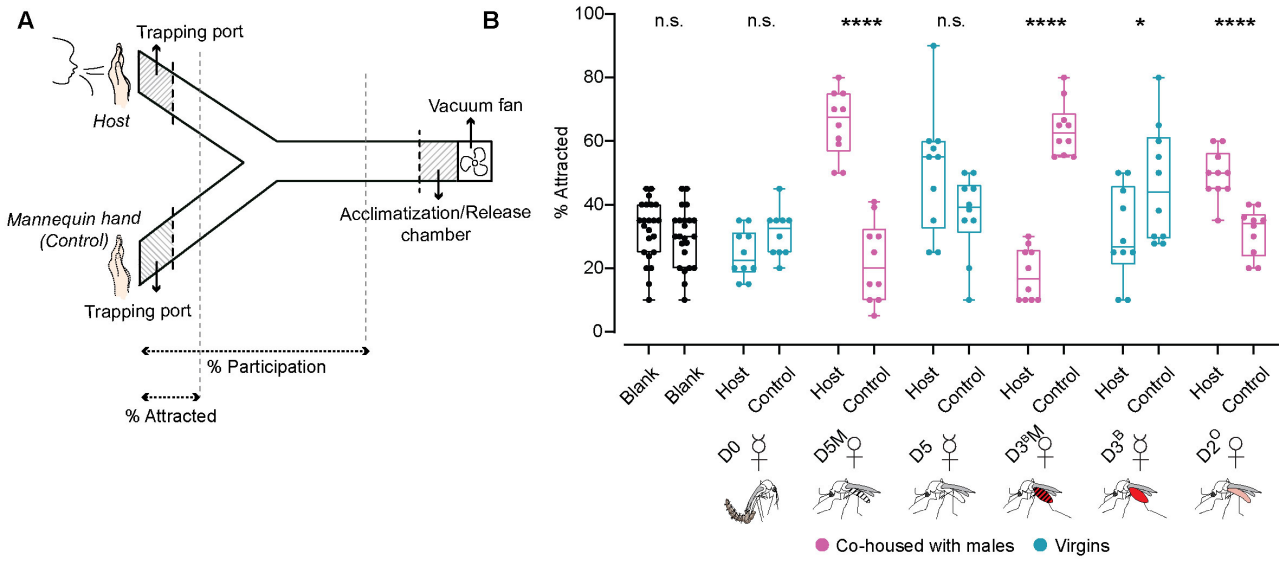

Fig. 2. Host-seeking is modulated like blood-feeding is in *An. stephensi*. A. Schematic of the Y-maze used to assess host-seeking behaviour of female *An. stephensi*. Females were allowed to acclimatise in the chamber for 5 minutes while being exposed to host kairomones that were presented in a test arm. A fan sucked the air from both host and control arms at 0.3-0.6m/s. Mosquitoes were released after acclimatisation and allowed to choose between the two arms. B. Percent females attracted to either host-cues or control arm at the indicated time points in the Y-maze. 17-21 females/trial, n=10 trials/group. Unpaired t-test, $p<0.05$. n.s. not significant, * $p<0.05$, ****$p<0.0001$. (D0: day of emergence ; D5M: 5days post-emergence, mated; D5: 5days post-emergence, virgin; $D3^{B}M$: 3days post-blood-meal, mated; $D3^{B}$: 3days post-blood-meal, virgin; $D2^{O}$: 2days post-oviposition)

ditions tested (cyan, figure 2B). Yet, like in the blood-feeding assay, blood-fed virgins were comparatively more attracted to human host-cues than were the mated blood-fed females (figure 2B).

These data suggest that, like blood-feeding, host-seeking is also modulated through the female's reproductive cycle, and mating influences this modulation by enhancing it initially and suppressing it post-blood-meal. The variability in response of virgin females suggests that mating enhances the female's initial attraction to a host.

Neurotranscriptomics reveals several candidate genes that promote blood-feeding. While sensitivity to host kairomones may modulate blood-feeding, it is also possible that central brain circuitry contributes to it. We reasoned that cues from mating, or signals from other tissues such as midgut could act on brain circuitry to modulate blood-feeding. To determine the molecular underpinnings of this behavioural modulation, we performed RNA sequencing from the midbrains of mosquitoes at different stages of their reproductive cycle (consequently different states of blood-deprivation or -satiety). This included females at emergence (D0), 5-days after emergence (D5; sugar-fed, blood-deprived), virgins and mated females one day after a blood-meal ($D1^{B}$, $D1^{B}M$), and females one day after oviposition ($D1^{O}$). Age-matched males were included for the earliest two time points (figure 3A).

For each of our samples, 81-87% of about 20-30million reads aligned to the *An. stephensi* genome (53). The variance between our replicates was low as represented in the Principal Component Analysis (PCA) (figure 3B). In PCA, older female brains, regardless of mating-, blood-feeding-, or oviposition- status clustered together while the youngest female and male brains stood apart on PC1 and PC2 suggesting that age and sex contribute most significantly to the variance in our data (figure 3B). The expression pattern of some hallmark genes showed the expected trends. Genes involved in eclosion behaviours – *eclosion hormone* (54) and *partner of bursicon*(55) – showed the highest expression in the D0 samples and were not expressed later. Male-specific genes, *HMG-B-13-like*, were expressed only in males (56), and genes involved in vitellogenic stages of egg-development – *vitellogenins*, *Ecdysone receptor*, and *E-20-monooxygenase*(57)– were expressed only in post-blood-meal samples (figure 3C).

We next explored this data for insights into the molecular underpinnings of blood-feeding modulation. Reports suggest that anticipatory metabolic changes in female germline cells and a 'vittelogenin wave' in fat bodies can drive specific appetite in *Drosophila* (58) and *Ae. albopictus* (34) respectively. However, we did not find any evidence for a similar anticipatory metabolic change that might drive blood-feeding in the mosquito brain (figure S2B). Interestingly, we found that after a blood-meal, glucose is neither spent nor stored, and that the female brain goes into a state of metabolic 'sugar rest', while actively processing proteins (figure S2B, S3). We similarly plotted genes involved in lipid metabolism, neurotransmitters, neuropeptides and their receptors and found no significant patterns (figure S4, S5, S6). In summary, contrary to our expectations, we saw no evidence for anticipatory metabolic changes in the brain that might in turn drive blood-feeding behaviour.

In an alternate approach to identifying genes that might modulate blood-feeding, we took the intersection of genes that

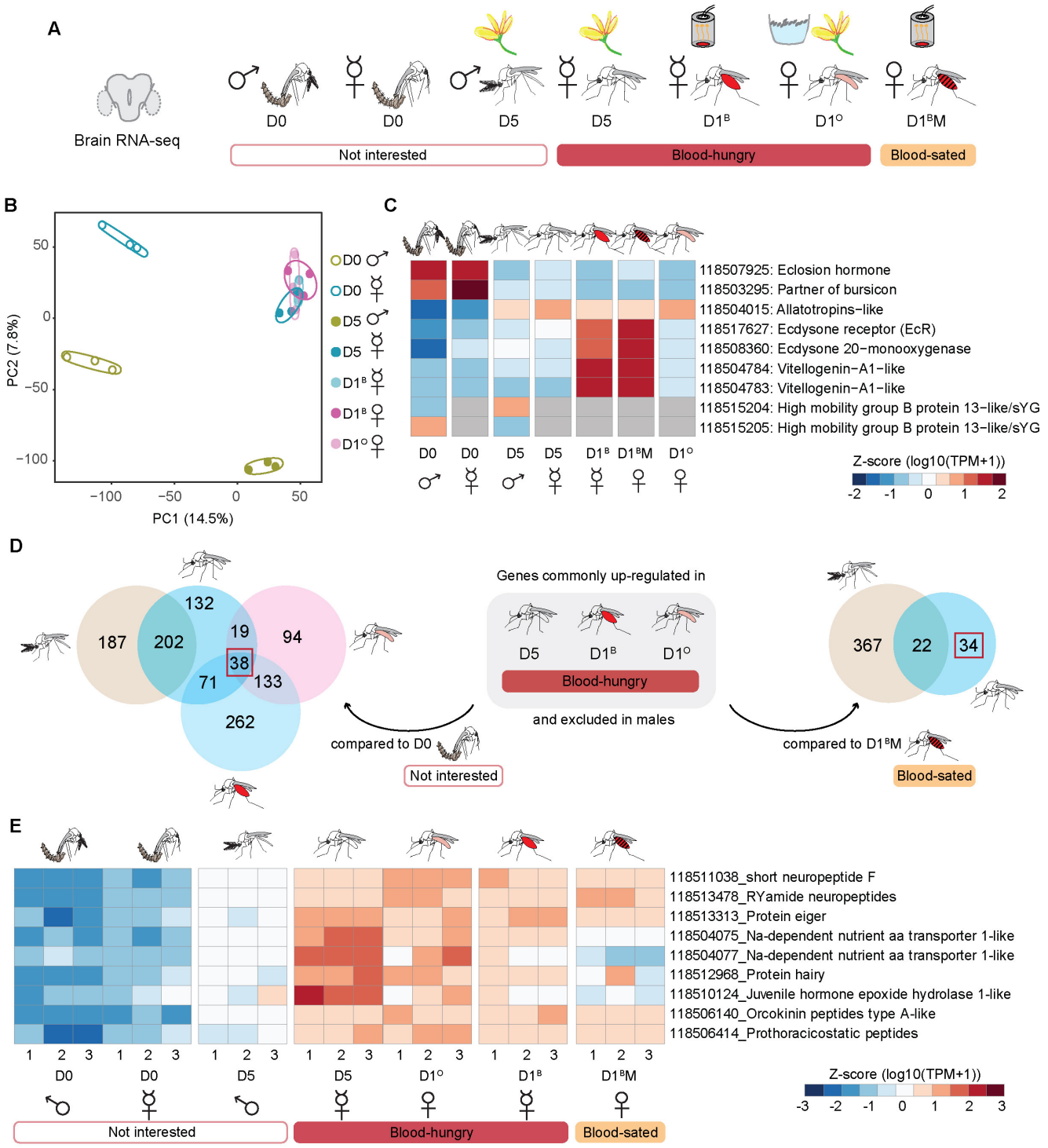

Fig. 3. Neurotranscriptome of *An. stephensi*. A. Midbrains were sampled from males and females at different ages and feeding preferences for bulk RNA-seq. Uninterested in blood: D0 males, D0 females, D5 males. Blood-hungry: D5, sugar-fed virgin females, $D1^B$ virgin females, and $D1^O$ females. Blood-sated: $D1^B$ mated females. n=100 midbrains per replicate; 3 biological replicates per sample, 7 samples. B. Principal Component Analysis (PCA) of the normalised counts-per-million from different brain RNA-seq samples. Replicates cluster closely, and age and sex contribute most to the differences between the samples. C. Genes (listed on the right) with known expression patterns plotted across different samples. These known expression patterns are reproduced in our data. Average of the triplicate data are represented as z-score normalised log10 (TPM+1) values. Grey cells represent no data. D. Identification of candidates potentially involved in promoting blood-feeding behaviour. Two types of comparisons were made: (left) genes commonly up-regulated in the three blood-hungry conditions (see figure 3A) when compared against D0 females and excluded in males, and (right) genes up-regulated in D5 sugar-fed virgin females when compared against $D1^B$ mated females (blood-sated), and excluded in males. Number of candidate genes identified from two different sets of analyses are boxed in red. E. Nine candidate genes (listed on the right), shortlisted for further validation. RNA-seq data from midbrain samples in triplicates are represented as z-score normalised log10 (TPM+1) values. (D0: day of emergence; D5: 5days post-emergence, virgin; $D1^B$: 1day post-blood-meal, virgin; $D1^B$M: 1day post-blood-meal, mated; $D1^O$: 1day post-oviposition)

were enriched in the three blood-hungry conditions (and absent in males). These comparisons were made against the two conditions that were not motivated to blood-feed: females at emergence and mated-blood-fed females (figure 3D). These shortlisted 38 and 34 genes respectively, gave us 68 unique candidates (excluding common genes and isoforms) that might promote blood-feeding in *An. stephensi* (figure S7).

Neuropeptides *sNPF* and RYamide promote blood--feeding in *An. stephensi*. We employed multiple, independent criteria while further short-listing candidates from the above analysis: 1) genes that showed the expected expression pattern: low in newly-emerged males and females; high in blood-hungry females; low in blood-sated females, 2) all neuropeptides, since these are known to regulate feeding behaviors, and 3) all genes related to juvenile hormone (JH) and 20-hydroxyecdysone (20E) signaling pathway, since they regulate development and reproduction in mosquitoes. This gave us 9 candidates (figure 3E): Two sodium-dependent amino acid transporters *118504075 and 118504077*. Transporters can sense nutrients and regulate feeding in *Drosophila* (29, 59). The neuropeptides included *Orcokinin (Ork)*, *Prothoracicostatic peptides (Prp)*, *RYamide (RYa)* and *short Neuropeptide F (sNPF)*, and a metabolic hormone *Eiger*, which responds to low nutrient conditions in *Drosophila* (60). *Protein Hairy* and *Juvenile hormone epoxide hydrolase 1-like (JHEH)* are involved in the JH pathway (61, 62)(figure 3E).

Using dsRNA, we knocked each of these genes down and tested their blood-feeding behaviour. In each case, we ensured efficiency of gene knockdown post-hoc (figure 4A). We first confirmed that the injection itself did not cause any behavioural changes (figure 4B) and in all following experiments either *dsGFP*-injected or uninjected females were included as controls.

We saw no change in behaviour upon loss of *Eiger*, *JHEH*, and *Ork* function (figure S8A-C, S8A'-C'). We were able to downregulate *Hairy* and *Prp* transcript levels by only 30-35%, hence cannot comment on their role in modulating blood-feeding (figure S8D, S8E, S8D', S8E'). Downregulation of the two transporters was efficient and resulted in a marginal reduction in blood-feeding (figure S8F, S8G, S8F', S8G'). However, their combined knockdowns, though effective, did not show any significant change in behaviour (figure S8H, S8H').

Two neuropeptides - *sNPF* and *RYa* - showed about 25% and 40% reduced mRNA levels in the heads but these animals showed no change in blood-feeding (figure S9B, S9C, S9E, S9F). We noticed, however, that many of these animals did not engorge and instead took smaller blood-meals (figure S9D, S9G). Given this, and since neuropeptides are known to act in concert (63), we tested the possibility that *sNPF* and *RYa* might act together to regulate blood-feeding behaviour. Indeed, their simultaneous dsRNA injections resulted in about 40% of the animals not taking blood-meals (figure 4C). Since RNA interference (RNAi) can be variable, and each female is an independent experiment, we pooled the females that took blood-meals and those that didn't separately before quantifying mRNA from them. We noted that knockdown efficiency was always higher in the heads of females that did not take blood-meals suggesting that downregulating these genes caused the suppression of blood-feeding (figure 4D). Importantly, we observed that sugar-feeding was unaffected in these females (figure 4C).

Since RNAi results in systemic knockdowns and neuropeptides are known to influence behaviour from their action in non-neuronal tissues such as the gut (38, 63, 64), we modified our dsRNA injection protocol to knock *sNPF* and *RYa* down in the abdomen while leaving their levels in the head unaltered (figure 4F, S9J, S9L). In this case we observed no change in blood-feeding behaviour (figure 4E, S9I, S9K). This suggests that the abdominal *sNPF* and *RYa* alone cannot influence blood-feeding and their action in the brain is necessary. Since the head knockdowns always also showed abdominal knockdowns (figure S9C, S9F) it is possible that the two neuropeptides act in both the brain and the gut to influence blood-feeding behaviour.

To determine in which cells *sNPF* and *RYa* act, we used hybridisation chain reaction (HCR) (65, 66) *in situ*. We found that they are expressed in several non-overlapping neuronal clusters distributed across many regions in the brain (figure 4G, S10A) and only in the Kenyon cells of the mushroom body were they were co-expressed (figure 4H, S10B). This is reminiscent of their expression in *Drosophila* and *Bombyx* (67–69). Importantly, we found a cluster of cells in the SOG that expresses *sNPF* only in the blood hungry-state (figure 4I, supplementary video). *sNPF* was either absent or diminished from this cluster in newly-emerged or sated females. Since the RNAi experiments suggested the abdominal involvement of these neuropeptides, we also looked for their expression in the midgut where we could detect only *sNPF*, not *RYa* (figure 4J, S11A, S11B, S11E). Interestingly, *sNPF* expression was also modulated in the midgut: there were more *sNPF* positive enteroendocrine cells (EECs) in the posterior midguts of blood-hungry females (figure 4K,L). Neuropeptides work by acting on their receptors to trigger downstream signalling cascades in the cells that express the receptors. We identified putative receptors for *sNPF* and *RYa* (see methods) and found that both were expressed in several overlapping cell-clusters in the brain (figure 4M, S10C, S10D). In the midgut, however, we could only detect *sNPFR* and not *RYaR* (figure 4M, S11C, S11D, S11F).

Together, these data suggest increased *sNPF* expression in both the brain and midgut might drive the blood-feeding behaviour, but that this occurs in the context of *RYa's* action in the brain.

Conclusions

The blood- and sugar-feeding behaviours of *An. stephensi* reported here share similarities and important differences with other mosquito species. For example, while mating is essential for the first blood-meal in *Aedes*, it is largely dispensable in *Anopheles*. How mating mediates behavioural

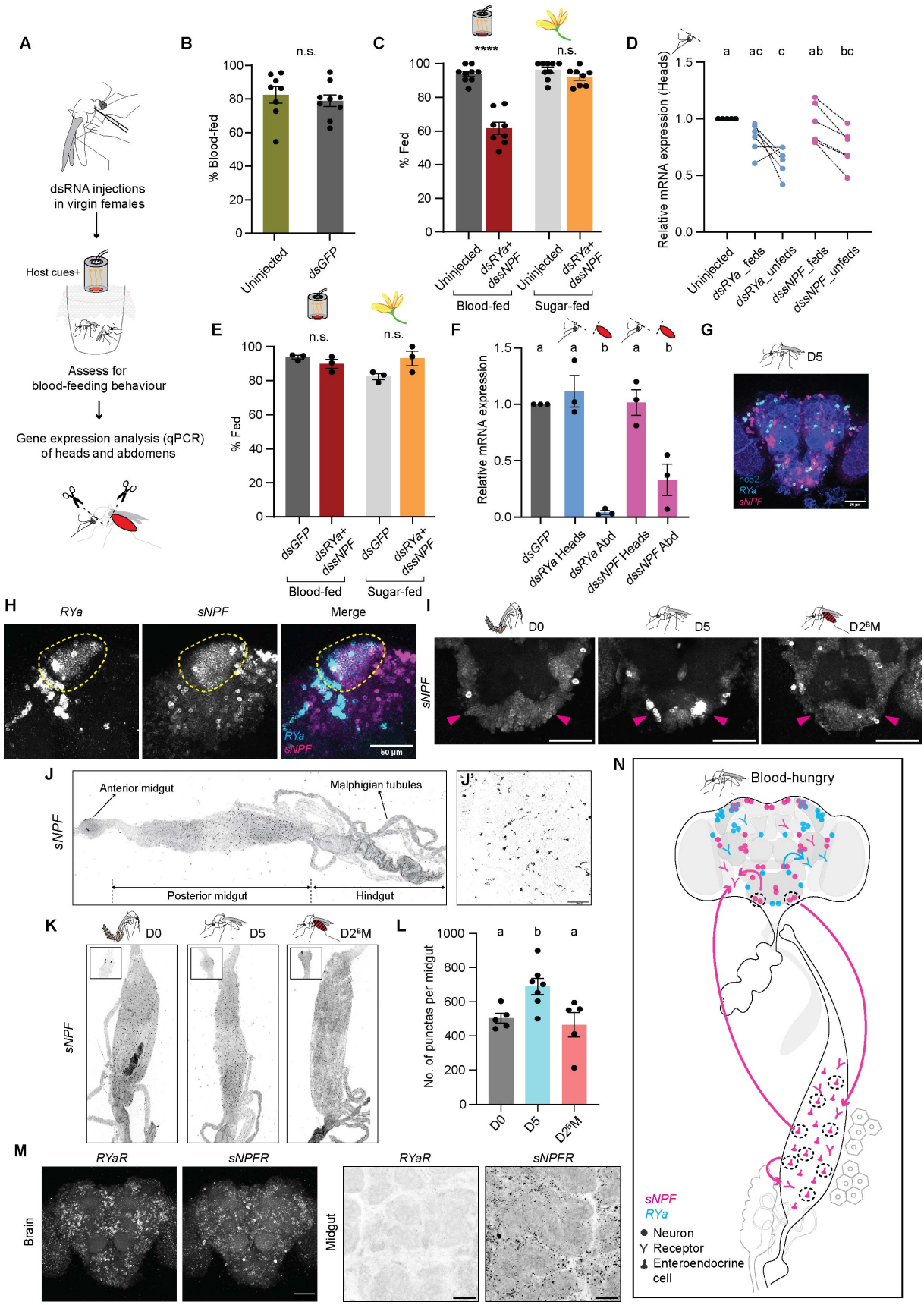
A
dsRNA injections
in virgin females
Host cues+
Assess for
blood-feeding behaviour
Gene expression analysis (qPCR)
of heads and abdomens
B
n.s.
% Blood-fed
Uninjected
dsGFP
C
****
n.s.
% Fed
Uninjected
dsRYa+
dssNPF
Blood-fed
Sugar-fed
D
a
ac
c
ab
bc
Relative mRNA expression (Heads)
Uninjected
dsRYa_feds
dsRYa_unfeds
dssNPF_feds
dssNPF_unfeds
E
n.s.
n.s.
% Fed
dsGFP
dsRYa+
dssNPF
Blood-fed
Sugar-fed
F
a
a
b
a
b
Relative mRNA expression
dsGFP
dsRYa Heads
dsRYa Abd
dssNPF Heads
dssNPF Abd
G
D5
nc82
RYa
sNPF
H
RYa
sNPF
Merge
RYa
sNPF
50 µm
I
D0
D5
D2BM
sNPF
J
Anterior midgut
Malphigian tubules
sNPF
Posterior midgut
Hindgut
J'
K
D0
D5
D2BM
sNPF
L
a
b
a
No. of punctas per midgut
D0
D5
D2BM
M
RYaR
sNPFR
Brain
RYaR
sNPFR
Midgut
N
Blood-hungry
sNPF
RYa
Neuron
Receptor
Enteroendocrine
cell

Fig. 4. short Neuropeptide F (sNPF) and RYamide (RYa) together promote blood-feeding in *An. stephensi*. A. Schematic representation of the pipeline used for functional validation. dsRNAs against candidate genes were injected in adult virgins for targeted RNAi. After recovery these were tested for blood-feeding. Knockdown efficiency was determined via qPCR in whole heads and abdomens of fed and/or unfed females after the behaviour. B. Comparison of uninjected females and *dsGFP*-injected females for blood-feeding behaviour revealed no difference between the two, indicating that the animals recovered from the injection procedure. 19-25 females/replicate, n= 8-9 replicates/group. Unpaired t-test, p<0.05. n.s. not significant. C,D. Blood-feeding and sugar-feeding behaviour of females when both *RYa* and *sNPF* are knocked down in the head (C). Relative mRNA expressions of *RYa* and *sNPF* in the heads of *dsRYa+dssNPF*- injected blood-fed and unfed females, as compared to that in uninjected females, analysed via qPCR (D). Simultaneous knockdown of both neuropeptides suppressed the blood-feeding behaviour of females, without affecting the sugar-feeding behaviour. Note the more efficient knockdown in the heads of unfed females, as compared to blood-fed females. 14-25 females/replicate, n=8-9 replicates/group. Unpaired t-test, p<0.05, ****p<0.0001, n.s. not significant (C). One way ANOVA with Holm-Šídák multiple comparisons test, p<0.05 (D). Data labelled with different letters are significantly different. E,F: Blood-feeding and sugar-feeding behaviour of females when both *RYa* and *sNPF* are knocked down only in the abdomen (E). Relative mRNA expressions of *RYa* and *sNPF* in the heads and abdomens of *dsRYa+dssNPF*- injected fed females, as compared to that in dsGFP-injected females, analysed via qPCR (F). No change in the blood-feeding or sugar-feeding behaviour was observed, despite the strong knockdown of both the genes in the abdomens, while the levels in the heads remain unaltered. 17-21 females/replicate, n=3 replicates/group.Unpaired t-test, p<0.05.n.s. not significant (E). One way ANOVA with Holm-Šídák multiple comparisons test, p<0.05 (F). Data labelled with different letters are significantly different. G, H. Whole mount mRNA *in situ* hybridisation of midbrain of 5days old sugar-fed virgin female, with *RYa* and *sNPF* probes (G). Both neuropeptides are expressed in multiple clusters (cyan: *RYa*, magenta: *sNPF*, blue: nc82). Co-expression was observed only in the Kenyon cells of the mushroom body (H). Maximum intensity projections of the confocal stacks are shown. Scale bar, 50µm. I. *sNPF* expression in the SOG region of the midbrains of females uninterested in blood (D0), blood-hungry females (D5) and blood-sated females ($D2^BM$). Note the appearance of a novel cluster only in the blood-hungry (D5) condition. Maximum intensity projections of selected confocal stacks are shown. Scale bar, 50µm. J. Whole mount mRNA *in situ* hybridisation of gut of 5days old sugar-fed virgin female with *sNPF* probes. *sNPF* expression was observed in the enteroendocrine cells (EECs) in the posterior midgut, shown in higher magnification in J'. Scale bar, 50µm. K,L. *sNPF* expression in the posterior midguts of females uninterested in blood (D0), blood-hungry females (D5) and blood-sated females ($D2^BM$). In addition to the EECs in the posterior midgut, two cells in the anterior midgut also show strong *sNPF* expression (K, inset). Higher number of cells express *sNPF* in the blood-hungry condition (L). n=5-7 guts per condition. M. Whole mount mRNA *in situ* hybridisation of midbrain (left) and midgut (right) of 5days old sugar-fed virgin female, with *sNPF receptor (sNPFR)* and *RYa receptor(RYaR)* probes. While both receptors are expressed in the brain, only *sNPFR* is expressed in the gut. Scale bar, 50µm. N. Summary schematic of *sNPF* and *RYa* function in modulating blood-appetite in *An. stephensi*. *RYa* and *RYaR* (cyan) are expressed only in the brain, while *sNPF* and *sNPFR* (magenta) are expressed both in the brain and the gut. Increased *sNPF* levels in both the tissues (dashed circles) promote a state of blood-hunger, which may drive feeding behaviour either by *sNPF's* action in the two tissues independently or via a communication between them. This happens in the context of *RYa* signalling in the brain. (D0: day of emergence; D5: 5days post-emergence, virgin; $D2^BM$: 2days post-blood-meal, mated)

changes is relatively well understood in flies: it is triggered by sex-peptide in the male semen, which modulates central brain circuitry (5, 7, 8, 70, 71) in the female. In mosquitoes, however, this is unlikely to be the case (72).

What then promotes blood-feeding? We have identified two neuropeptides: *RYa* and *sNPF* that act synergistically to do this in *An. stephensi*. Our data suggests that an increase in *sNPF* levels in the brain - likely released by a cluster of neurons in the SOG - as well as in the midgut, promotes a state of blood-hunger. Communication between the gut and the brain (and indeed between other tissues) has been noted to control feeding behaviour in many contexts (63, 73). For example, gut-derived NPF can act on the brain to promote increased protein intake in flies (64). We found that the receptor for *sNPF* is expressed both in the brain and gut and so cannot comment on whether the two tissues communicate with each other via *sNPF*, or each computes the heightened *sNPF* signal locally to contribute to the blood-appetite.

It is possible that *sNPF* promotes blood-feeding independent of *RYa*. However, we were unable to knock *sNPF* down completely to test this. Its synergistic requirement with *RYa*, despite no apparent modulation of *RYa* or its receptor, could result from a general state of hunger that *RYa* promotes, in the context of which, we were able to uncover the blood-feeding role of the diminished *sNPF*. Since many neurons co-express these receptors, it is possible that neurons downstream of *sNPF* or *RYa* expressing neurons integrate the two inputs to modulate behaviour. Our findings are in contrast with reports in *Aedes*, where *sNPF* and *RYa* suppress host-seeking (35, 36, 38). Instead, gut-derived neuropeptide-F (NPF) promotes host-seeking in *Aedes* (38). The contrasting roles of these neuropeptides in regulating blood-feeding in these two species highlights another important difference between them.

The female mosquito's dietary choices present a striking model in which to study the molecular and circuit control of feeding choices. While progress in this domain has been steady, with the parallel revolutions in novel technologies in genomics, circuit inquiry, and functional genetics, it will now be possible to scale these efforts and dissect this behaviour at cellular and molecular resolution.

Acknowledgements

This work was supported by the Tata Trust. We wish to acknowledge the insectary and its staff at TIGS. All sequencing was done at the Next Generation Genomics Facility (NGGF) at the Bangalore Life Science Cluster. All imaging was done at the Central Imaging and Flow Cytometry Facility (CIFF) at the Bangalore Life Science Cluster. We are grateful to Nitin Gupta, Mahul Chakraborty, Tussar Saha, Sriram Narayanan, Farah Ishtiaq, Kavita Isvaran, Sunil Laxman, Chris Q Doe, Claude Desplan, Krishna Melnattur, Suresh Subramani, K. VijayRaghavan, the Indian Neurobehaviour group, and the Vosshall lab for their invaluable input and discussion during the course of this project and comments on the manuscript.

Author contributions

PB conceptualised the project, performed all experiments except RNA-seq and host-seeking assay, performed all analysis, including RNA-seq, wrote and reviewed the manuscript. RP performed the RNA-seq experiments and analysis, standardised HCR, and reviewed the manuscript. PDB performed the host-seeking assay, provided technical assistance during HCR standardisations and determination of mating status, and reviewed the manuscript. SQS conceptualised and supervised the project and wrote and reviewed the manuscript.

Declaration of interests

None of the authors have any competing interests to declare.

Methods

Mosquito culture. *Anopheles stephensi* (Indian strain; Bangalore strain, TIGS-1) and *Aedes aegypti* (Bangalore collection) were reared in BugDorm cages and maintained at 26-28°C, 70-80% relative humidity with a photoperiod of 12h light: 12h dark. All the behavioural assays were performed at these conditions of temperature and humidity. Larvae were fed on a mixture of yeast and dog biscuit (1:3 ratio) and cultured in trays in appropriate densities to prevent overcrowding. Adult mosquitoes were provided *ad libitum* access to 10% sugar solution (8% sucrose +2% glucose +0.05% methyl paraben +5% vitamin syrup (Polybion SF Complete, Merck Ltd.)) at all times, unless specified otherwise. Females were provided O+ve human blood, secured periodically from blood banks, both for general maintenance and feeding assays.

Regulatory permissions. This project was approved by the Institutional Human Ethics Committee (Ref: inStem/IEC-22/02) and the Institutional Biosafety Committee (TIGS/M-7/8/2020-1).

Blood-feeding assay: first blood-meal, 0-120h post-emergence (D0-D5). All *An. stephensi* feeding experiments were performed from ZT12-ZT15 and *Ae. aegypti* experiments from ZT10-ZT12 (Zeitgeber time 0 is defined as the time of lights ON).

0-7h old mosquitoes were cold anesthetised and collected during the day in 1100ml paper cups covered with a net and secured with a rubber band. These were maintained at the conditions of temperature and humidity described above. To collect virgins, males were separated at the time of collection. 20 females with males (1:1 ratio) or without males were collected for each trial and were aged appropriately with *ad libitum* access to 10% sugar solution (supplementary figure S1A).

Females were assayed for their blood-feeding behaviour from the day of emergence (D0, 0-7h old) to 5 days of age (D5), every 24h. They were provided constant access to sugar, except when they were offered blood. A detailed schematic has been shown in figure S1A. On the day of the test, appropriately aged females were offered a blood-meal via a Hemotek feeder (Hemotek Ltd), which was maintained at 37°C and perfumed with human skin odours. It has been reported that female mosquitoes need to be 'activated' to take blood-meals. This involves the presentation of CO2 (and other host-cues) to the females, likely because CO2 has been shown to gate temperature and visual cues (74, 75). So, prior to offering the blood-meal, the mosquitoes were 'activated' by the presentation of a hand placed above the cup for 5 minutes, followed by 3 exhalations from the experimenter. Additionally, blood was supplemented with 1mM ATP (Sigma A6419) before loading the feeder (figure 1B). Females were allowed to feed for 60-90mins in dark and abdomens were scored visually for presence of blood, irrespective of the amount ingested (inset, figure S1A). For D0, no sugar was provided at the time of collection. Females were allowed to acclimatise for at least 30 mins in the cups and then offered a choice of both sugar and blood simultaneously, to assess their preference for blood soon after emergence (figure S1A).

In the case of co-housed females, males and females were housed together from the time of collection until the day of the experiment. Males were separated post-hoc and spermathecae of the females were dissected to score for the presence or absence of sperm (figure 1G). All the assays with virgin and co-housed females were performed in parallel by a single experimenter. Mosquitoes from at least 4 independent batches were tested for each day of the experimental timeline.

For *Ae. aegypti*, both virgin and mated females (mating status was confirmed via post-hoc dissection of spermathecae and all co-hosued females were found to be mated, data not shown) were tested for first blood-meal at only 8days post-emergence (D8, figure 1C). Behavioural experiments were performed the same way as described for *An. stephensi*.

Blood-feeding assay: second blood-meal, 24-96h post-first blood-meal ($D1^B$-$D4^B$). To ensure that the second blood-meal is not driven due to an incomplete first blood-meal, we selected only fully-engorged females to test for subsequent feedings (figure S1A). 5days old *An. stephensi* (both virgins and co-hosued with males) and 7-9days old *Ae. aegypti* (mated, as previously determined) were fed on blood and fully fed females were separated and collected in paper cups as described above. As a female takes about 2 days to digest blood, the second blood- meal ingested 24h post-first blood-meal ($D1^B$) was detected by the presence of Rhodamine B (Sigma R6626), which fluoresces in the red range (figure S1A). Spiking the second blood-meal with Rhodamine B (0.04µg/µL of blood) allowed visualisation of the freshly ingested blood, without affecting the feeding efficiency (supplementary figure S1B-D). To assess feeding at subsequent days ($D2^B$-$D4^B$), abdomens were dissected to differentiate between the bright red freshly ingested blood from the dark and clotted first blood-meal. In the case of co-housed *An. stephensi* females, spermathecae were not dissected to confirm mating as females were presumed to be mated when collected for this assay (5days old and co-housed with males for the entire duration from the time of emergence), as previously determined in figure 1G.

To confirm whether mating suppresses subsequent feeding (figure 1H), fully fed virgins were collected and allowed to mate for 3-4 days with aged-match males. No males were introduced in the virgin-only controls. Blood-feeding assay was performed as described above. Spermathecae were dissected post-hoc to determine the mating status and unmated females were not considered for the final analysis. Datasets with less than 80% total mating were discarded.

Blood-feeding assay: post-oviposition, 24-48h post-egg laying ($D1^O$-$D2^O$). For blood-feeding behaviour post-oviposition, fully fed females were separated and a water cup lined with moist paper (ovipositor) was provided for egg laying 2days post-blood-meal (determined in a separate assay described below, supplementary figure S1E;

figure S1A). Females were allowed to lay eggs overnight. The following morning, non-gravid females were visually identified by their lean bellies and separated in cups. Blood-feeding assay was performed the same evening for 1day post-oviposition ($D1^O$) and the following day ($D2^O$), as described above. Females were dissected post-hoc and scored for absence of mature ovaries, as a sign of successful oviposition. Gravid females were not considered for the analysis.

Determination of oviposition timing for *An. stephensi*. To determine the day of maximum oviposition, 5-6days old females co-housed with males were fed on blood, as described above. Fully fed females were separated and collected in BugDorm cages in groups of 10 females/cage. An ovipositor was provided the same day and females were allowed to lay eggs overnight. Eggs laid were counted the next day and a fresh ovipositor was provided. This cycle was repeated for the next 5 days. Total eggs laid each day were divided by the number of females present at the time of counting (supplementary figure S1E).

Sugar-feeding assay for *An. stephensi*. As mosquitoes feed on sugar in small bouts, as opposed to a replete blood-meal, we assessed sugar-feeding behaviour of females in windows of 24h for each test day. 0-7h old mosquitoes were collected during the day, separated in cups and aged appropriately. They were given access to 10% sugar solution at all times, as described above, except for the day of emergence (D0) when no sugar was provided at the time of collection (similar to the blood-feeding assay performed at D0).

To assess their sugar-feeding behaviour on the day of emergence (D0), 0-7h old females were acclimatised in the cups for 1h and sugar spiked with Rhodamine B (1mg/25ml of sugar; Sigma R6626) was presented for 2.5-3h. The fluorescence of Rhodamine B in the red channel allowed visualisation of even the tiniest amounts of sugar ingested by a female (figure S1G). For D1 feeding, 3-10h old females (with access to normal sugar so far) were then provided with Rhodamine B-sugar and allowed to feed on it for 24h. For D2 feeding, 27-34h old females (with access to normal sugar so far) were fed on Rhodamine B-sugar for the next 24h and scored as D2. This cycle was repeated until D5. In the case of co-housed females, males were separated post-hoc and spermathecae of the females were dissected to score for the presence or absence of sperm (figure S1H).

To assess sugar-feeding post-blood-meal, females fully fed on blood were collected and separated in cups, as described above. They were allowed to feed on Rhodamine B-sugar for 24h following a blood-meal and scored as $D1^B$. The next set of females (with access to normal sugar so far) were then provided with Rhodamine B-sugar from 24h-48h post-blood-meal and scored as $D2^B$. This cycle was repeated until 4 days post-blood-meal ($D4^B$, figure 1E).

For sugar-feeding post-oviposition, blood-fed females were provided an ovipositor 3 days later and were forced to oviposit during daytime by artificially creating dark conditions. Oviposited females (non-gravid) were then visually identified, separated and presented with Rhodamine B-sugar for the following 24h and scored as $D1^O$. The next set (with access to normal sugar so far) was then provided with Rhodamine B-sugar, 24-48h post-oviposition and scored as $D2^O$(figure 1E). For each day tested, females were dissected post-hoc and scored for absence of mature ovaries, as a sign of successful oviposition. Gravid females were not considered for the analysis.

Dual choice assay of blood and sugar. Mosquitoes were collected as described above. Males and females were co-housed for 4-6days with *ad libitum* access to sugar. To assess the choice between sugar and blood, mosquitoes were either given continuous access to normal sugar (sugar-sated) or starved with water 24h prior to the assay (sugar-starved). At the time of the assay, post-activation (as described above), blood and Rhodamine B-spiked sugar (1mg/25ml of sugar, Sigma R6626) were provided in parallel. After 60mins, abdomens were scored visually for ingestion of blood under white light, and under fluorescent microscope (red channel) for ingestion of sugar (figure S1F). Co-housed males served as an internal control for sugar-feeding. As males are unable to feed on blood, they were only scored for presence or absence of Rhodamine B-spiked sugar. Results are presented in figure 1F.

Statistical analysis of feeding behaviours. Statistical analysis was performed using GraphPad Prism (v10.2.0). To compare the blood-feeding and sugar-feeding behaviours of virgins and co-housed females in figure 1D, E, each day was treated as an independent experiment and p-values were computed for each pair-wise comparison.

Y-maze olfactory assay for host-seeking behaviour in *An. stephensi*. . A 30inch Y-maze was constructed as per the WHO guidelines (https://www.who.int/publications/i/item/9789241505024). Each arm of the Y-maze had a trapping port, while the stem was attached to a holding port. Each port had a mesh screen at one end, while the other was fitted with a sliding door to trap or release mosquitoes. The holding port was attached to a fan which pulled air from the two arms, over the mosquitoes, and out at a velocity of 0.3-0.6m/s. Optic flow information (alternate black and white stripes) was placed underneath the Y-maze to act as visual guide for navigation.

Following conditions were tested: D0 virgins, D5 sugar-fed virgins, D5 sugar-fed mated females (D5M), 3days post-blood-meal virgins ($D3^B$), 3days post-blood-meal mated females ($D3^BM$), and 2days post-oviposition females ($D2^O$). For mated conditions, females were co-housed with males for 5days post-emergence and assumed to be mated based on our previous findings (figure 1G). For each condition, mosquitoes were collected and provided *ad libitum* access to sugar as described above. Females were transferred to holding ports 7-8h prior to the assay and were starved during this time with only access to water. For each run, mosquitoes were acclimatised for 5 minutes: 2 min with clean air and 3 minutes

with an experimenter presenting a hand at one of the arms and simultaneously exhaling at resting rates. To account for disruption in airflow, the hand of a mannequin was placed at the other arm (control). Post-acclimatisation, the door of the holding port was opened to release the mosquitoes and they were allowed to make a choice for 5 minutes in the presence of continued host-cues. The ports were then closed and mosquitoes in each arm counted. All the mosquitoes trapped in a port, sitting on the door or resting on the half-length of the Y-arm were considered as "attracted" to that stimuli (host or control, figure 2A). Participation percentage was also calculated as number of mosquitoes that passed half-way through the Y-stem/total number of mosquitoes released (figure S1I).

Several controls were included to avoid experimental artefacts. Each experimental day started with a blank trial (where no stimuli were presented on either arm of the Y-maze) and the side of the host-cues presentation was alternated with each trial to eliminate side biases. Trials for blood-fed virgins and mated females were done both in parallel and on multiple days to eliminate the influence of external factors which might be present on a given day. When testing blood-fed females, aged-matched sugar-fed females (blood-hungry) were included as positive controls where ever possible, with satisfactory results. Lastly, we made sure that at least 50% of the mosquitoes had made either choice in all runs, except for D0 (newly emerged females) and blank runs. In the rare cases that this was not true, we did not consider those for the analysis. Statistical analysis was performed using GraphPad Prism (v10.2.0). To compare the attraction of females to host-cues and control in figure 2B, each time-point was treated as an independent experiment and p-values were computed for each pair-wise comparison.

Bulk RNA sequencing of midbrains and data analysis. For bulk RNA sequencing, midbrains were dissected from the following conditions: D0 and D5 sugar-fed males; D0 and D5 sugar-fed virgin females; 1day post-blood-meal virgin ($D1^B$) and mated females ($D1^BM$) and 1day post-oviposition females ($D1^O$). For post-blood-meal conditions, 5days old females were fed on blood and fully fed females were separated for sample preparation. Females co-housed with males for 5 days were assumed to be mated based on our previous findings (figure 1G). Three replicates from independent batches were prepared for each condition.

Mosquitoes were cold anesthetised before dissections. Brains were dissected in RNase-free 1X PBS and immediately placed into ACME solution (13:3:2:2 of water, methanol, acetic acid, and glycerol) on ice, which mildly fixes the tissues (76). For each condition, 100 brains were dissected per replicate. The mildly fixed brains were washed with cold 1X PBS and centrifuged at 13,000 rpm for 5 min at 4°C to remove ACME. Brains were then homogenised in TRIzol (Invitrogen), flash-frozen, and stored at -80°C until RNA extraction. RNA was extracted using Direct-zol RNA MicroPrep (Zymo Research) columns. RNA quantity and quality were assessed using the ThermoFisher Qubit 4 and RNA 6000 Nano kit Bioanalyser, respectively.

The cDNA library was prepared for each sample using the NEBNext Ultra II Directional RNA Library Prep kit (Catalog no-E7765L), with an average fragment size of 250 bp. Some of the library samples were subjected to size and quality checks using a bioanalyser. Paired-end sequencing was carried out on the Illumina Hiseq 2500 sequencing platform, generating 2×100 bp reads. The library preparation and sequencing were performed at the Next Generation Genomics Facility (NGGF) at Bangalore LifeScience Cluster.

Post-sequencing, samples were demultiplexed and delivered as raw Fastq files. After passing the quality check using the FastQC tool, the reads were mapped onto the reference *An. stephensi* transcriptome (NCBI RefSeq assembly GCF013141755.1) (53) using Kallisto v0.43.1 (77) with default parameters. 81-87% of reads aligned to the mosquito transcriptome.

Transcript-level abundance was quantified using Kallisto and gene-level summarisation was performed using the Tximport function in R, with transcript isoform information retained. Using the EgdeR package, the raw counts were converted to Counts Per Million (CPM) and log2 transformed before data filtering (genes with less than 1 CPM in at least 3 or more samples were filtered out) and normalisation, using the trimmed mean of M-values (TMM) method. Principal component analysis (PCA) was performed using the prcomp function in R and visualised using the ggplot function. Data was checked for batch effects using gPCA (78) in R and the test statistic "delta" was found to be 6.957686e-05, with a p-value of <0.001, indicating no batch-effects.

Differential gene expression analysis

Differential expression analysis was performed using the Limma package in R. A design matrix was created to specify the sample conditions, and the Voom function was used to estimate the mean-variance relationship across genes. A linear model was then fitted to the data using the mean-variance relationship. Bayesian statistics were calculated for the data by creating a contrast matrix to extract the linear model fit. To identify differentially expressed genes (DEGs), the "decideTests" function was used by applying a fold change threshold of 2 (or log fold change of 1) and a FDR (false discovery rate) adjusted p-value cutoff of 0.05. The number of genes identified to be upregulated and downregulated in each pair-wise comparison are shown in figure S2A.

To plot Transcripts Per Million (TPM) values as heatmaps, the Fastq files for the midbrain samples were mapped onto the reference *An. stephensi* transcriptome and abundance was quantified using Kallisto the same way as described above. Gene-level summarisation was done using Tximport as described above, except all the isoforms of a given transcript were mapped to a single gene. The resultant TPM values were first filtered for TPM>0.1 in each sample. Next, the genes that were not quantified in at least 2 of the 3 replicates of each sample group were removed. The filtered dataset were then log10 transformed and heatmaps were plotted using the pheatmap function in R. To construct heatmaps of

genes involved in carbohydrate and lipid metabolism (supplementary figure S3, S4), key enzymes of the respective canonical pathways were manually curated based on the existing literature. Fat body, midgut and ovary data (SRX620223, SRX618937 and SRX620224; bioproject SRP043489) for 2-4days old, sugar-fed *An. stephensi* females were taken from Prasad et al.(79). Fastq files were downloaded from the SRA explorer and processed similarly.

Gene set enrichment analysis

eggNOG mapper tool 2.1.9 (80) (parameters: 70% identity and minimum 70% query coverage) was used to find functionally annotated orthologs of the identified DEGs in *An. gambiae*.*An. gambiae*-specific orthologs were fed into the GOSt tool from gProfiler2 (81) toolset for functional enrichment analysis. A custom gene list comprising of all the genes identified in our RNA-seq experiment was provided as a background instead of the whole genome. Using this background, an ordered query was run with an FDR adjusted p-value threshold of 0.05 to determine which GO terms (Biological Processes) were over-represented. This was done for all sets of DEGs and the top 10 terms of each set were plotted using ggplot function in R (figure S2B).

dsRNA-mediated gene knockdown. To synthesise the double-stranded RNA (dsRNA), coding regions (500-600bp) of candidate genes were amplified from cDNA of *An. stephensi* females using forward and reverse primers with T7 promoter sequence at 5' ends. The gel purified fragments were then used as a template for *in vitro* transcription reactions using Megascript RNAi kit (Invitrogen) or High-Yield T7 RNAi Kit (Jena Biosciences) as per the manufacturers' protocols. The dsRNAs were purified using the phenol-chloroform method and pellet dissolved in nuclease-free water. The dsRNA for green fluorescent protein (GFP) was synthesised from plasmid pAC5.1B-EGFP (Addgene 21181) to be used as a negative control for off-target effects of dsRNA-mediated knockdown.

Virgins were collected for injections as described above. The day and concentration of dsRNA to be injected was determined for each target gene individually. *dsEiger*: injected in 24h old virgins at 5-6µg/µL; *dsHairy*: injected in 24h old virgins at 4-5µg/µL; *dsJHEH*: injected in 72h old virgins at 5µg/µL; *dsPrp*: injected in 72h old virgins at 3-5µg/µL; *dsOrk*: injected in 96h old virgins at 5µg/µL; *ds118504077* and *ds118504075*: 96h old virgins at 6µg/µL. To achieve tissue-specific knockdown of *sNPF* and *RYa*, injections were performed at different days: in 0-10h old virgins (4µg/µL or 7µg/µL) to achieve abdomen-specific knockdowns and in 96h old virgin females (7µg/µL) to achieve knockdowns in both head and abdominal tissues. For dual injections, purified dsRNAs were mixed in equal amounts to a total of 7µg/µL and injected on the day previously determined.

Injections were performed on a FemtoJet 4i system (Eppendorf) and each female was injected with 0.5-0.6µL of the respective concentrated dsRNAs in the upper thorax. In some cases, dsRNAs were also injected in the abdomens to ensure that the site of injection does not alter the behaviour. Uninjected or *dsGFP*-injected (same concentration as that of the candidate gene) females were included as a control each time. 15-25 females were injected for each trial and at least 2 trials from independent batches of mosquitoes were performed for each target gene.

Injected females were allowed to recover in paper cups with *ad libitum* access to sugar and assessed for blood-feeding behaviour at 3 days post-injection, as previously described. Fed and unfed females were visually scored and whole heads and abdomens were collected separately for analysis. Total RNA was extracted using Direct-zol RNA MicroPrep (Zymo Research) columns, as per the manufacturer's protocol. RNA was quantified using Qubit Broad range assay (Invitrogen). For each sample, 200-220ng RNA was used to prepare cDNA using the SuperScript™ IV Reverse Transcriptase (Invitrogen 18090050) or Maxima H Minus Reverse transcriptase (Thermo Scientific EP0752). Quantitative PCR (qPCR) was performed using PowerUp™ SYBR™ Green Master Mix (Applied Biosystems) to determine the knockdown efficiency. Relative mRNA abundances were calculated using the delta-delta Ct method (82), normalised to RpS7. Statistical analyses were performed using GraphPad Prism (v10.2.0).

To assess the sugar-feeding behaviour of dsRNA injected females (*dssNPF*, *dsRYa* and *dsRYa+sNPF*), injections were performed as described above. Injected females were allowed to recover with *ad libitum* access to normal sugar for the first two days, which was then replaced with Rhodamine B-spiked sugar (1mg/25ml of sugar, Sigma R6626) for the next 24h. Control females were treated similarly. The blood-feeding assay was performed 3 days post- injection as described above, with both blood and sugar provided in parallel. Abdomens were scored visually for ingestion of blood under white light, and under fluorescent microscope (red channel) for ingestion of sugar (figure S9A).

Hybridisation chain reaction (HCR). Previously published protocol (83) was modified to perform HCR *in situ* hybridisations on brain and gut tissues collected from females under three different conditions: D0 (not interested in blood), D5 virgins (blood-hungry) and $D2^B$, mated (blood-sated). All the reagents, including the probes, amplifiers and buffers were procured from Molecular Instruments Inc. A set of custom-designed 20 probe pairs were used per target gene: *sNPF (118511038)*, *RYa (118513478)* and their receptors. To find *sNPF* and *RYa* receptors in *An. stephensi*, putative protein sequences were blasted against orthologs in *Drosophila melanogaster*, *Ae. aegypti* and *An. gambiae*. Based on high identities, consistent in all three organisms, *118517381* and *118507167 (NPY receptor type 2)* were identified as *RYa receptor (RYaR)* and *sNPF receptor (sNPFR)* respectively.

5-7 brains for each target, per condition were dissected in ice cold PBS and fixed with 4% PFA (in PBS) for 20 minutes at room temperature. Post-washing steps with PTw (0.1% Tween-20 in PBS), 4 times 10 mins each, tissues were permeabilised using detergent solution (50mM Tris-Cl, pH7.5,

150mM NaCl, 1mM EDTA, pH8, 0.5% Tween-20, 1% SDS) for 30 mins at room temperature. Brains were then pre-hybridised in probe hybridisation buffer for 30 mins at 37°C, followed by incubation with neuropeptide probes (0.8pmol each) at 37°C for 48h in a humid chamber. Samples were washed with pre-warmed wash buffer, 4 times 15 mins each, at 37°C to remove unbound probes. This was followed by 2 washes, 5 mins each with 5X SSCT (0.1% Tween-20 in 5X SSC) at room temperature. Samples were then pre-amplified using amplification buffer for 30 mins at room temperature. For each sample, 2µL (3µM stock) of each hairpins were mixed and prepared by heating at 95°C for 90secs for annealing. They were allowed to cool to room temperature for 30mins in a dark chamber and 100µL amplification buffer was added to the mix. Brains were incubated in the hairpin solution for 12-16h at 37°C in dark and excess hairpins were washed off with multiple 5X SSCT washes: twice for 5 mins, twice for 30mins, once for 5 mins. For nc82 staining, all the steps were performed in 0.5% PTw buffer (0.5% Tween-20 in PBS). Brains were equilibrated in 0.5% PTw and incubated with anti-mouse nc82 (1:200; DSHB, RRID: AB2314866) for three overnights at 4°C. Post-washing, goat anti-mouse Alexa-fluor405 (1:400, Invitrogen) was added and samples were left in dark, for one-two overnights at 4°C. After washing off the unbound secondary antibody, samples were equilibrated for at least an hour in Vectashield and mounted in Vectashield for imaging. *In situs* against neuropeptide receptors were performed the same way, except the washing steps to remove the unbound probes were performed at 42°C and samples were incubated with the hairpin solution at room temperature (to minimise background). As controls for background signal, samples were prepared the same way, except no probes were added in the hybridisation buffer (figure S10E). Samples for all three conditions were dissected, processed and imaged the same day.

Protocol for gut *in situs* was adapted from Slaidina et al.(84). 5-8 gut samples for each target, per condition were dissected in ice-cold PBS and fixed with 4% PFA (in PTw) for 20 minutes at room temperature. Post-washing steps with PTw, tissues were dehydrated on ice with graded methanol washes: 25% methanol (in PTw), 50% methanol (in PTw), 75% methanol (in PTw) and 100% methanol for 10 mins each. Samples were stored in 100% methanol for up to a month, at -20°C. For rehydration, samples were washed sequentially with graded methanol: 75% methanol (in PTw), 50% methanol (in PTw), 25% methanol (in PTw), followed by a wash in permeabilisation solution (1% Triton-X in PBS). Samples were permeabilised for 2h at room temperature and fixed again with 4% PFA (in PTw) for 20 minutes. Following 10mins washes: washed once with PTw, twice with 50% PTw/50% 5X SSCT and twice with 5X SSCT, samples were pre-hybridised in probe hybridisation buffer for 30 mins at 37°C, followed by incubation with probes (0.8pmol each) at 37°C for 48h in a humid chamber. Post washing steps with wash buffer at 37°C and 5X SSCT at room temperature, samples were pre-amplified in amplification buffer for 30 mins at room temperature. Hairpins were prepared the same way as described above and samples were incubated in hairpin solutions for 12-16h in dark at room temperature. Following 2 washes 5 mins each with 5X SSCT, samples were incubated with DAPI (1:1000 in 5X SSCT) for one hour at room temperature. Samples were washed with 5X SSCT, 4 times, 10mins each and equilibrated in Vectashield for at least an hour before mounting. As controls for background signal, samples were prepared the same way, except no probes were added in the hybridisation buffer (figure S11G, H). Samples for different conditions, prepared on different days and stored at -20°C, were processed and imaged together. Statistical analyses were performed using GraphPad Prism (v10.2.0).

All samples were imaged at Central Imaging and Flow Cytometry Facility (CIFF) at NCBS. Images were acquired with a 40X/1.3NA or 10X/0.4NA (whole guts) objectives at a resolution of 512X512 pixels, on an Olympus FV3000 system. Images were viewed and manually analysed using ImageJ/FIJI (85). Maximum intensity projections of all z-stacks in an image are shown, except in figures 4H, 4I, S10B, S10D, where stacks were manually selected to capture relevant brain structures.

Supplementary Figure S1

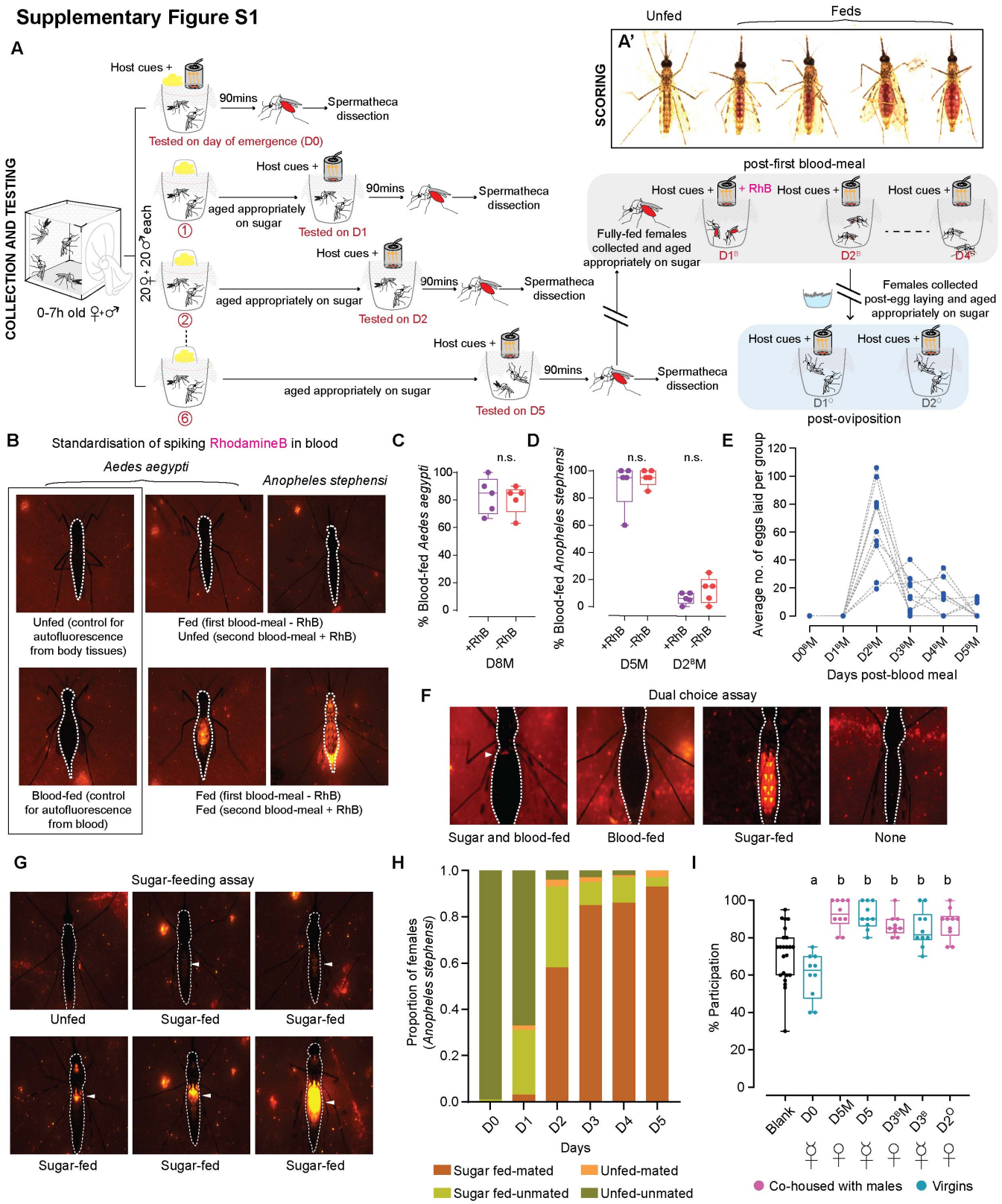

Supplementary Figure 1. Standardization of various behavioural assays to study feeding behaviours in *An. stephensi* A. Detailed schematic of the assay designed to assess the blood-feeding behaviour of virgins and co-housed females across the reproductive cycle. 0-7h old mosquitoes were collected and about 20 females (with or without 20 males) were separated into cups. Each cup was aged appropriately and tested on the relevant day (see methods for more details). Number of blood-fed mosquitoes were visually scored, irrespective of the quantity fed. Representative images of differently fed females are shown in A'. Females were tested for first blood-meal from the day of emergence (D0) to five days of age, every 24h. Spermathecae of co-housed females were dissected post-hoc to determine the mating status. To assay for the second blood-meal, fully fed females were collected and aged appropriately in groups of 20. To assess feeding 1day post-first blood-meal ($D1^B$), Rhodamine B was spiked in the second blood-meal offered to the females. The subsequent days ($D2^B$-$D4^B$) were tested without any such spiking (grey box; see methods for more details). To assay for blood-feeding behaviour in females after oviposition ($D1^O$-$D2^O$), freshly oviposited females were collected and aged in groups of 20 for the appropriate time in cups (blue box; see methods for more details). In all cases, females were presented with host-cues prior to the assay and testing was performed as shown in figure 1B (see methods for more details). B. Standardisation of spiking Rhodamine B dye in blood to assess feeding 24h post-first blood-meal ($D1^B$). To assay for the second blood-meal, blood-fed females were collected, aged for 24h and offered Rhodamine B-spiked blood in a Hemotek. All other assay parameters remained the same as for the first blood-meal (see methods for more details). Widefield fluorescent images of *Ae. aegypti* and *An. stephensi* fed on second blood-meal spiked with Rhodamine B are shown. Images on the left (black box) show mosquitoes not fed and fed on un-spiked blood (without Rhodamine B), as controls for autofluorescence from body tissues and blood itself, respectively. Fluorescence from Rhodamine B added to the second blood-meal enabled identification of fresh blood intake in previously fed mosquitoes reliably. C,D. Comparison of feeding behaviours of *Ae. aegypti* females (C) and *An. stephensi* females (D) fed on blood with and without Rhodamine B at the indicated age. Females fed similarly on both indicating that Rhodamine B itself does not affect feeding behaviour. Unpaired t-test, $p<0.05$. n.s not significant. 16-20females/trial. n= 5 trials/group. D5M: 5days post-emergence, mated; $D2^B$M: 2days post-blood-meal, mated; D8M: 8days post-emergence, mated). E. Determining optimal oviposition timing in *An. stephensi*. Females were tested in groups of 10 and average number of eggs laid per group are shown at the indicated day after the first blood-meal. Dashed lines connect the eggs laid by each group on the indicated day. Majority of the eggs were laid 2days after blood-meal. 10 females/group, n=10 replicates/group. $D0^B$-$D5^B$M: 0-5days post-blood-meal, mated. F. Standardisation of the dual choice assay, to determine the choice between blood and sugar in sugar-sated and sugar-starved *An. stephensi* females, co-housed with males. Widefield fluorescent images of females fed on either blood, sugar or both are shown. White arrowhead marks the fluorescence from sugar (spiked with Rhodamine B) in the abdomens of females engorged on blood, indicating that the female has fed on both. This is not observed in the females fed on blood alone. Females fed on sugar alone can be visualised by the fluorescent lean bellies. Unfed females exhibit no fluorescence or engorgement. G. Widefield fluorescent images of female *An. stephensi* fed on sugar spiked with Rhodamine B. This setup was used to study the sugar-feeding behaviour of virgins and co-housed females across the reproductive cycle. Addition of Rhodamine B to standard sucrose solution enabled visualisation of even the smallest amounts ingested, as indicated by the white arrowheads, under the fluorescent microscope. H. Mating status of sugar-fed and sugar-unfed co-housed females tested in figure 1E, 24-120h post-emergence (D0-D5). n=175-179 females per time-point. I. Percent participation of virgin and co-housed females tested for host-seeking behaviour in the Y-maze olfactometer (figure 2B), at different stages of the reproductive cycle. All females tested participated well. 17-21 females/trial, n=10 trials/group. Kruskal-Wallis, with Dunn's multiple correction test, $p<0.05$. Data labelled with different letters are significantly different.D0: day of emergence ; D5M: 5days post-emergence, mated; D5: 5days post-emergence, virgin; $D3^B$M: 3days post-blood-meal, mated; $D3^B$: 3days post-blood-meal, virgin; $D2^O$: 2days post-oviposition.

Supplementary Figure S2

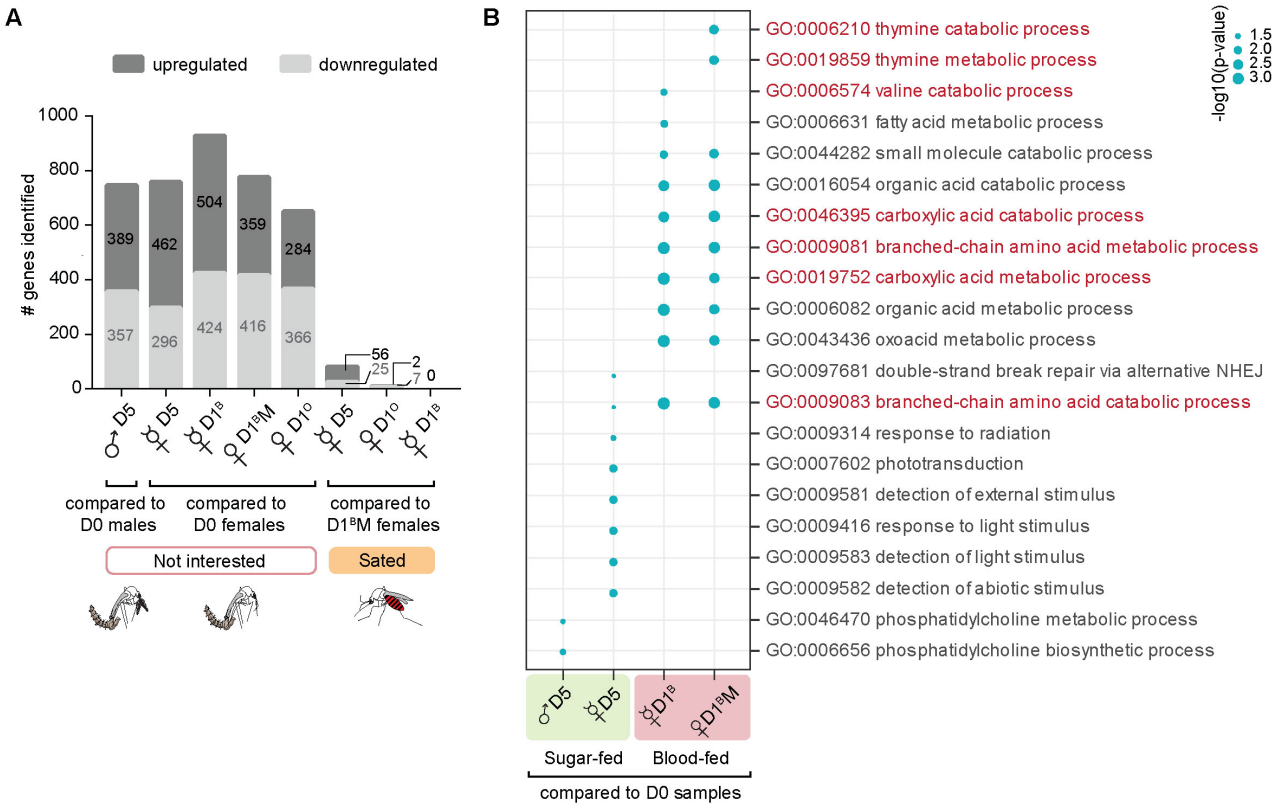

Supplementary Figure 2. Differential expression of genes across various states of blood-hunger and -satiety.. A. Number of genes identified to be differentially up- and down-regulated in the midbrain of females across the reproductive cycle (indicated at the bottom), compared to either newly emerged males or females (D0), or blood-fed sated females ($D2^{B}M$). Note that no genes were found to be differentially expressed between mated and virgin blood-fed females, despite their contrasting blood-appetites. B. Top 10 Gene Ontology terms for Biological Processes (GOBP), overrepresented in the samples indicated at the bottom, compared to newly emerged males or females (D0). Size of the dot indicates the p-value significance. Processes involved in protein metabolism (highlighted in red) were found to be highly enriched in blood-fed females. (D0: day of emergence; D5: 5days post-emergence, virgin; $D1^{B}$: 1day post-blood-meal, virgin; $D1^{B}M$: 1day post-blood-meal, mated; $D1^{O}$: 1day post-oviposition)

Supplementary Figure S3

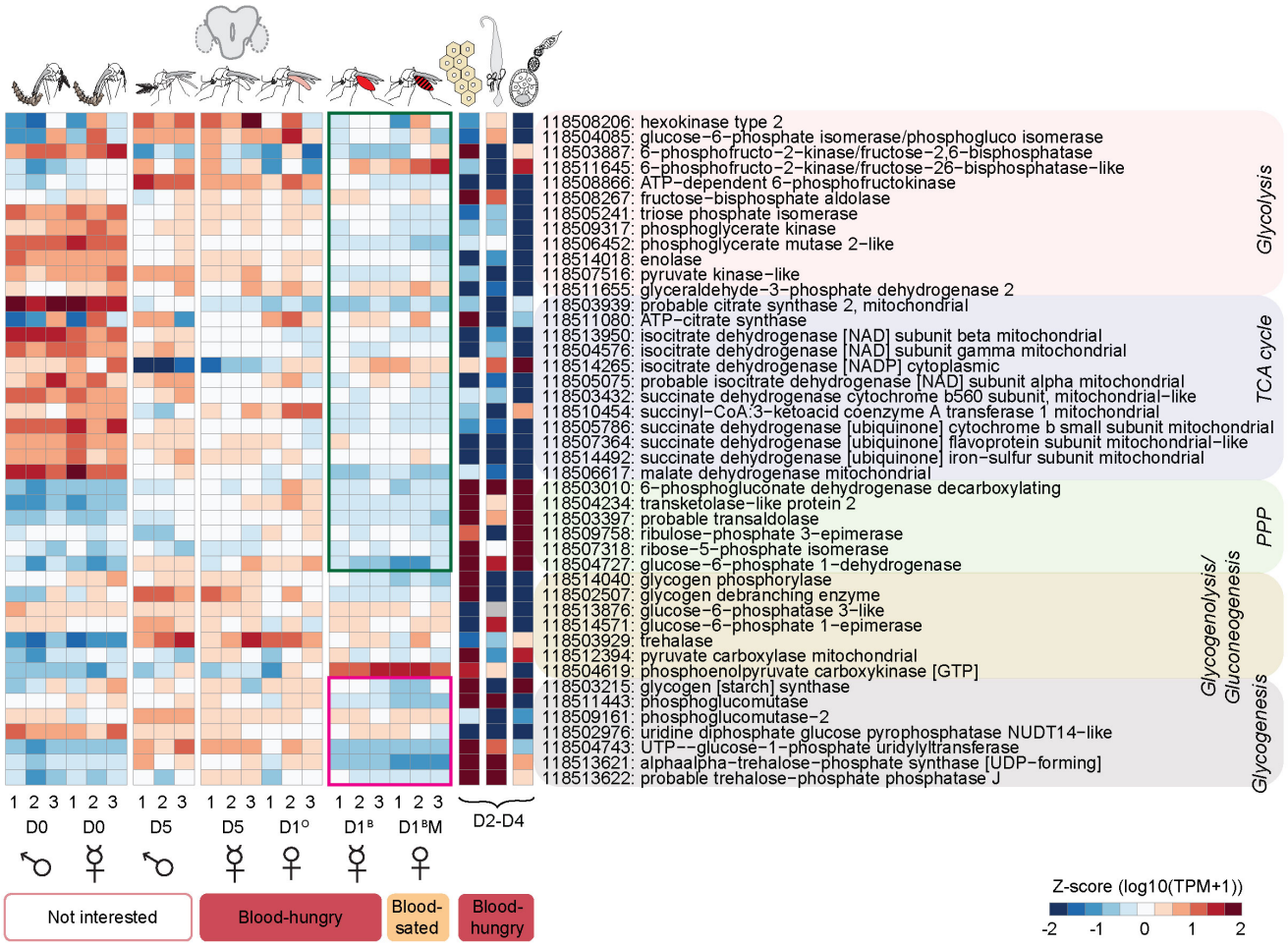

Supplementary Figure 3. Differential expression of genes involved in carbohydrate metabolism across different tissues and states of blood-hunger and -satiety in *An. stephensi* Expression patterns of genes (listed on the right) involved in sugar metabolism via different pathways, across the reproductive cycle in the midbrain and in the fat body, midgut and ovary of blood-hungry females, are represented as heatmaps. Green box shows downregulation of genes involved in glucose utilisation and the magenta box represents genes involved in glucose storage. Note that both are low in the brains of blood-fed females indicating that the brain goes into a state of 'sugar rest' after a blood-meal. Analysing publicly available data from the midgut, ovary, and fat body of sugar-fed females suggest that energy expenditure via the non-oxidative branch of the pentose phosphate pathway of glucose metabolism is high in these tissues, likely to prime them for the blood-meal. RNA-seq data from all midbrain samples in triplicates and single sample data for fat body, midgut and ovary (taken from Prasad et al., 2017) are represented as z-score normalised log10 (TPM+1) values. Grey cells represent no data. (D0: day of emergence; D2-D4: 2-4days post emergence; D5: 5days post-emergence, virgin; $D1^{B}$: 1day post-blood-meal, virgin; $D1^{B}M$: 1day post-blood-meal, mated; $D1^{O}$: 1day post-oviposition)

Supplementary Figure S4

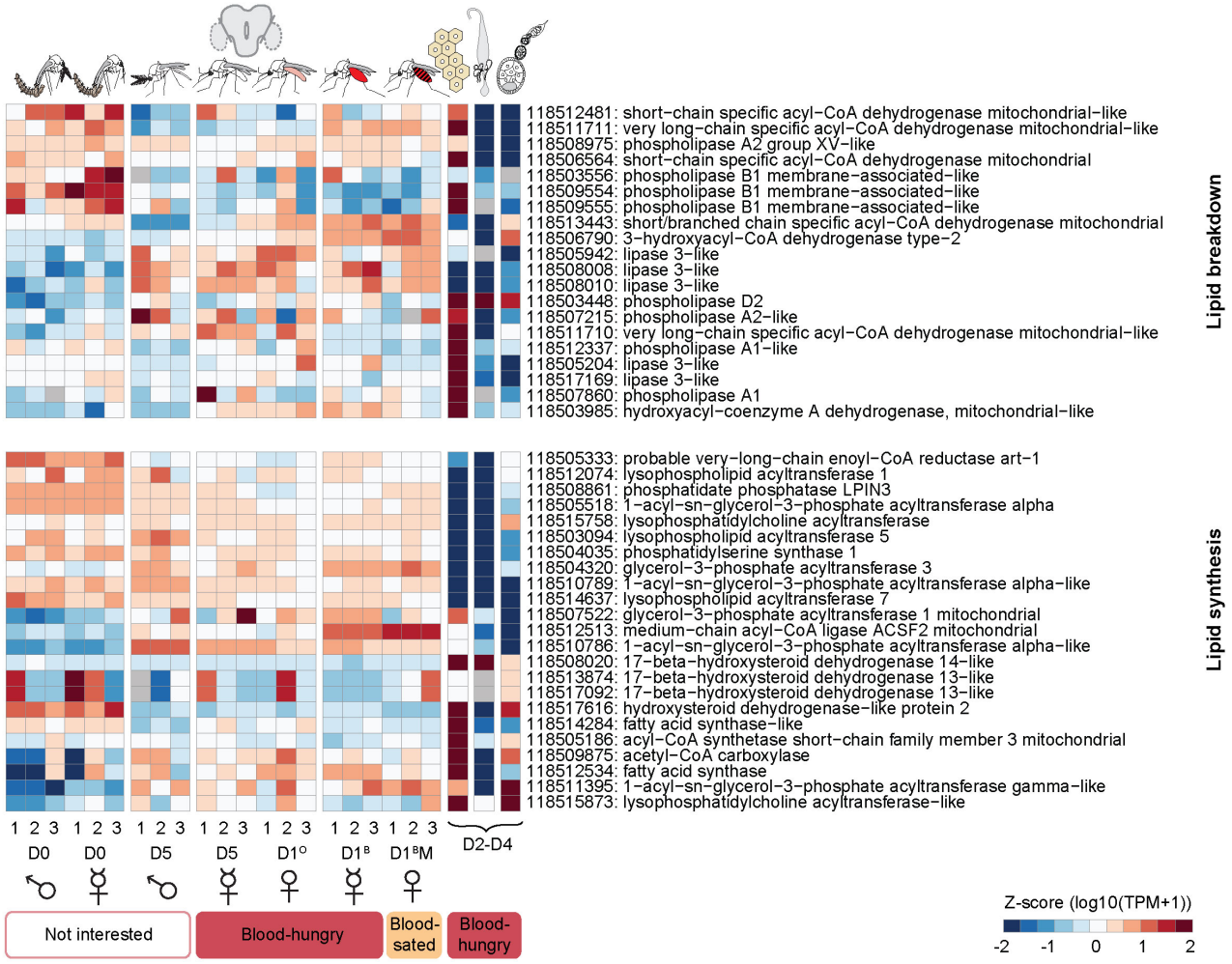

Supplementary Figure 4. Differential expression of genes involved in lipid metabolism across different tissues and states of blood-hunger and -satiety in *An. stephensi*. Expression patterns of genes (listed on the right) involved in lipid metabolism: lipid breakdown (top) and lipid synthesis (bottom), across the reproductive cycle in the midbrain and in the fat body, midgut and ovary of blood-hungry females, are represented as heatmaps. No specific patterns were observed in the midbrains (pre- and post-blood-meal), midgut or ovaries. As expected, fat body showed high expression of genes involved in both the catabolic and anabolic branches of fatty-acid metabolism. RNA-seq data from all midbrain samples in triplicates and single sample data for fat body, midgut and ovary (taken from Prasad et al., 2017) are represented as z-score normalised log10 (TPM+1) values. Grey cells represent no data. (D0: day of emergence; D2-D4: 2-4days post emergence; D5: 5days post-emergence, virgin; $D1^{B}$: 1day post-blood-meal, virgin; $D1^{B}M$: 1day post-blood-meal, mated; $D1^{O}$: 1day post-oviposition)

Supplementary Figure S5

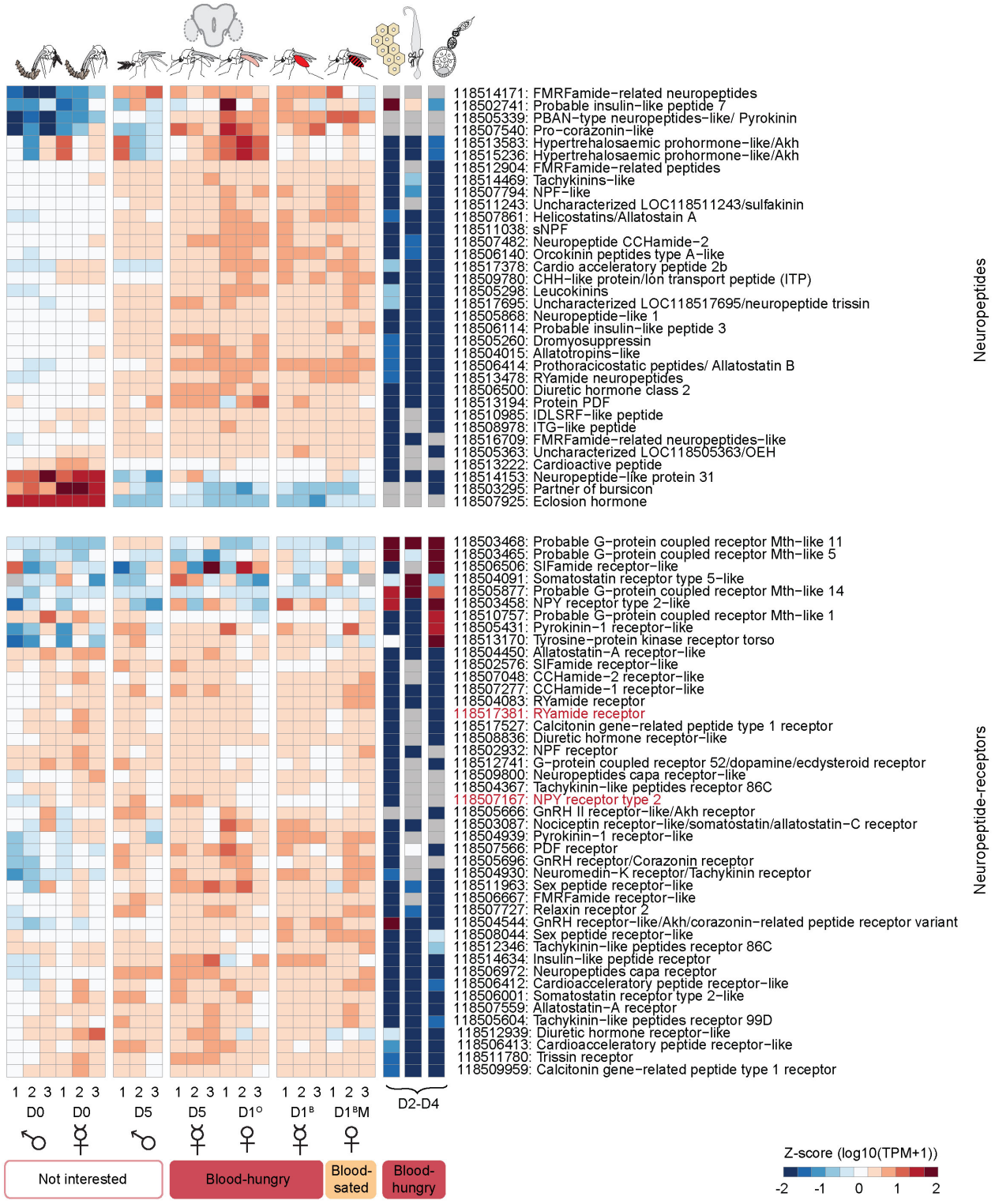

Supplementary Figure 5. Expression patterns of neuropeptides and neuropeptide-receptor across different tissues and states of blood-hunger and -satiety in *An. stephensi*. Expression patterns of neuropeptides (top) and neuropeptide-receptors (bottom), across the reproductive cycle in the midbrain and in the fat body, midgut and ovary of blood-hungry females, are represented as heatmaps. While neuropeptides were observed to be downregulated in the midbrains of newly emerged males and females (D0), neuropeptide-receptors showed no such patterns. Additionally, both neuropeptides and their receptors were much more abundant in the brain, as compared to fat body, midgut or ovaries. Transcripts for the receptors highlighted in red were visualised *in situ* both in the midgut and brain samples via HCR (figure S10, S11). RNA-seq data from all midbrain samples in triplicates and single sample data for fat body, midgut and ovary (taken from Prasad et al., 2017) are represented as z-score normalised log10 (TPM+1) values. Grey cells represent no data. (D0: day of emergence; D2-D4: 2-4days post emergence; D5: 5days post-emergence, virgin; $D1^B$: 1day post-blood-meal, virgin; $D1^BM$: 1day post-blood-meal, mated; $D1^O$: 1day post-oviposition)

Supplementary Figure S6

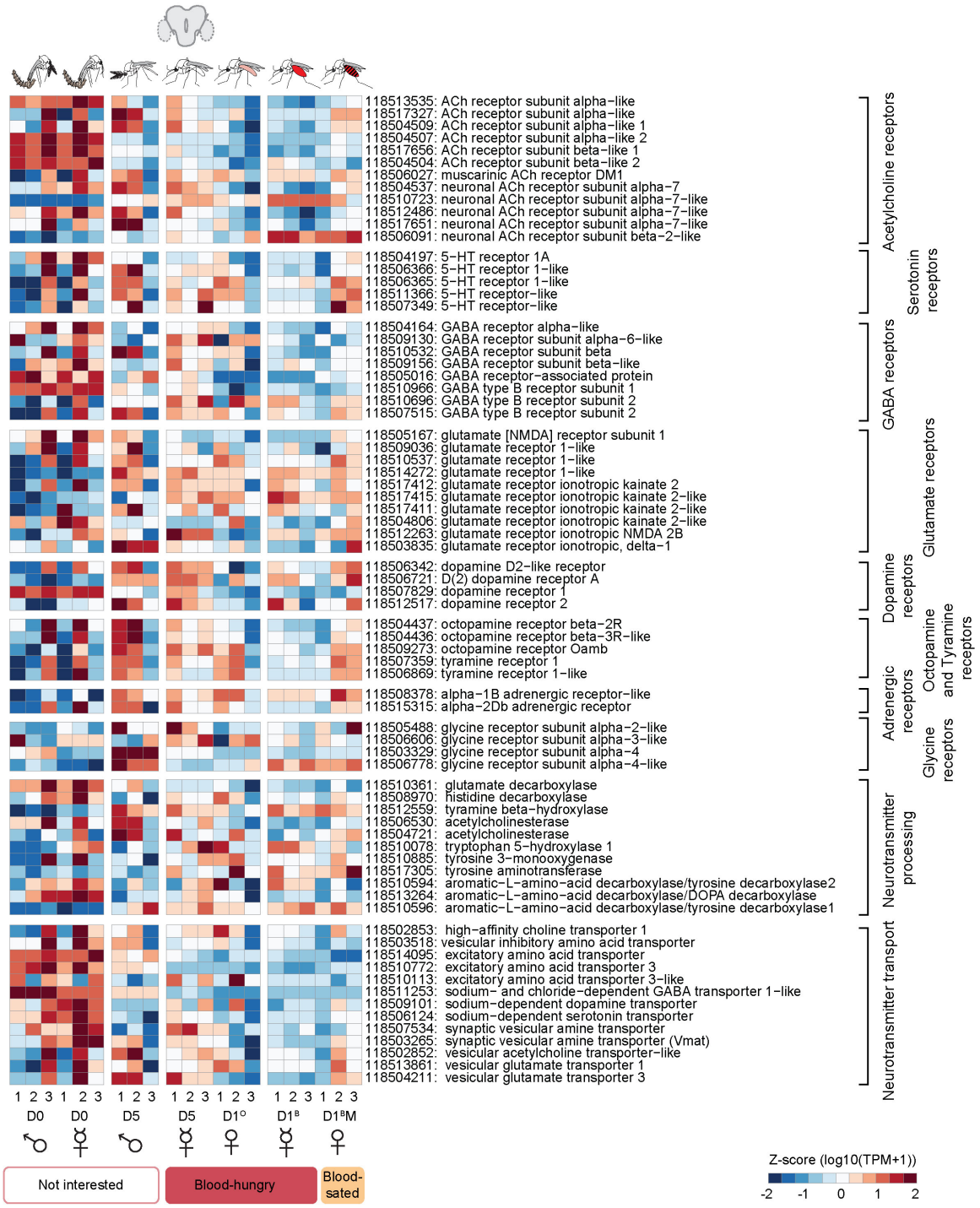

Supplementary Figure 6. Expression patterns of neurotransmitter-related genes in the midbrain of *An. stephensi* across different states of blood-hunger and -satiety. Expression patterns of genes (listed on the right) involved in neurotransmitter expression, processing and transport across the reproductive cycle in the midbrain, are represented as heatmaps. Interestingly, many of these genes were observed to be up-regulated in the newly emerged (D0) mosquitoes as compared to the older and blood-fed mosquitoes. RNA-seq data from all midbrain samples in triplicates are represented as z-score normalised log10 (TPM+1) values. (D0: day of emergence; D5: 5days post-emergence, virgin; $D1^B$: 1day post-blood-meal, virgin; $D1^BM$: 1day post-blood-meal, mated; $D1^O$: 1day post-oviposition)

Supplementary Figure S7

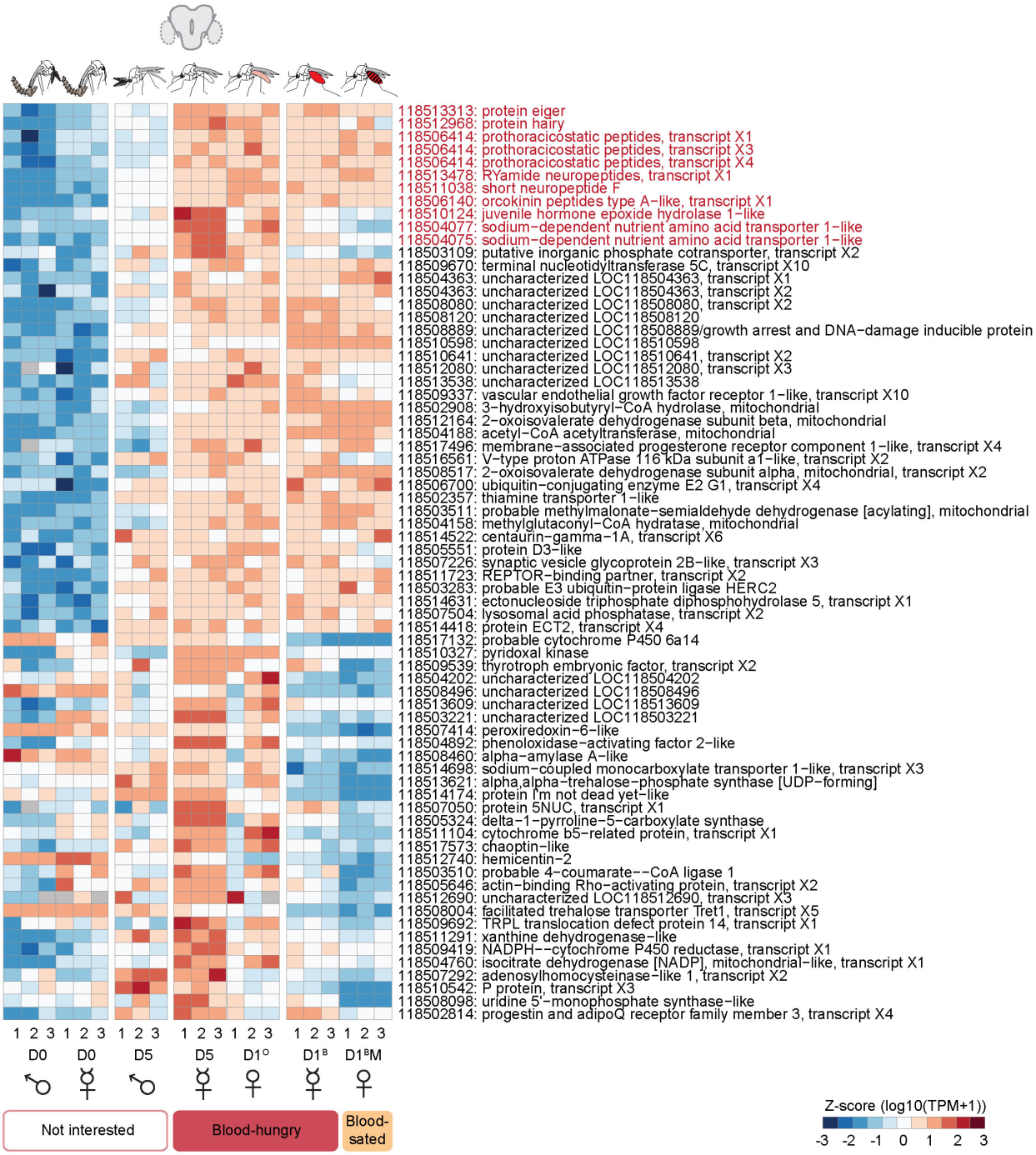

Supplementary Figure 7. Candidates potentially involved in promoting blood-feeding behaviour in *An. stephensi*. 71 candidate genes identified as potential promoters of blood-feeding are listed. These were identified to be commonly up-regulated in different conditions of blood-hunger (as compared to conditions of satiety or no-interest), and non-overlapping in males. Nine genes shortlisted for further validation are highlighted in red. RNA-seq data from all midbrain samples in triplicates are represented as z-score normalised log10 (TPM+1) values. Grey cells represent no data. (D0: day of emergence; D5: 5days post-emergence, virgin; $D1^{B}$: 1day post-blood-meal, virgin; $D1^{B}M$: 1day post-blood-meal, mated; $D1^{O}$: 1day post-oviposition)

Supplementary Figure S8

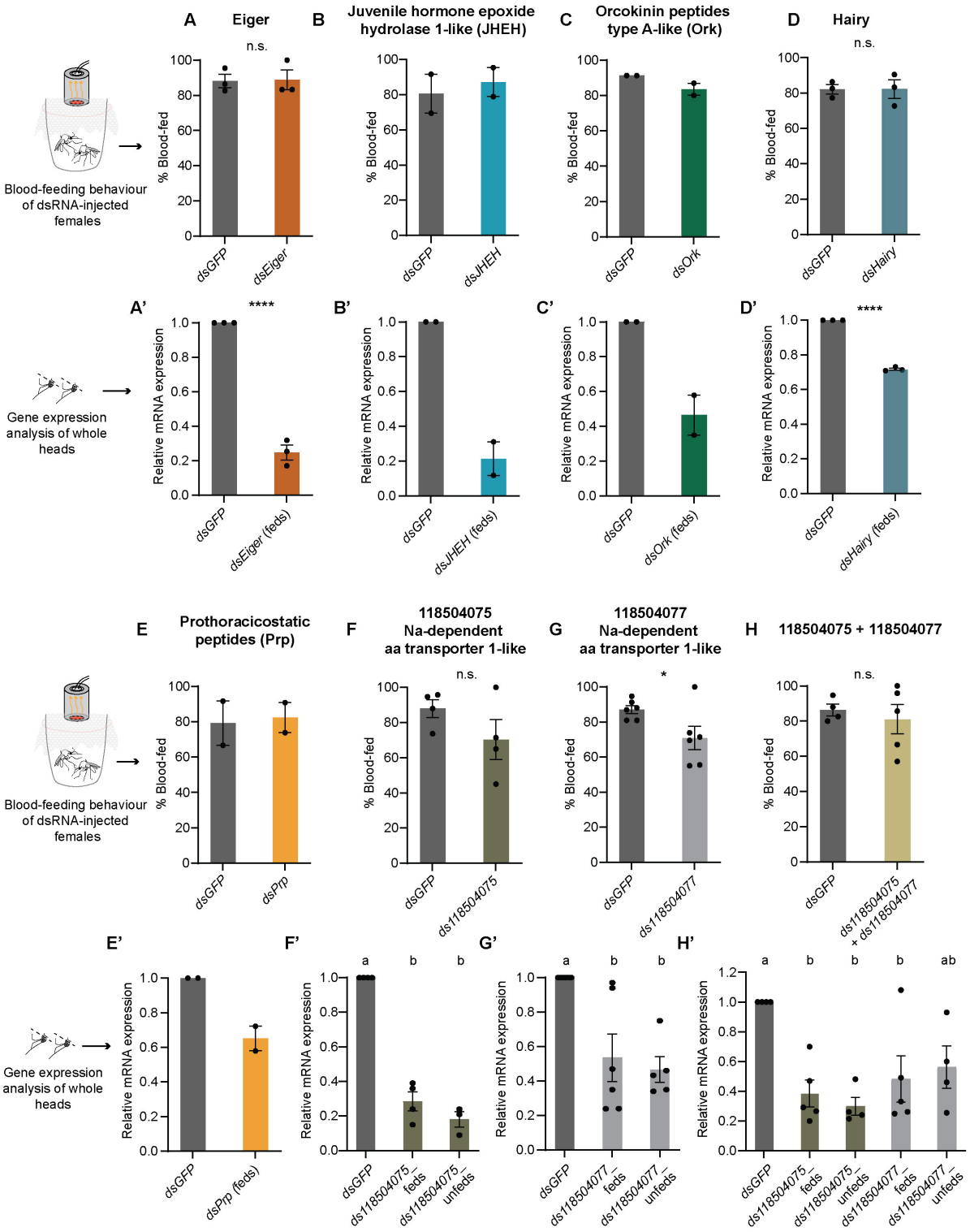

Supplementary Figure 8. Screening of the shortlisted candidates, potentially involved in promoting blood-feeding behaviour in *An. stephensi* via dsRNA-mediated gene knockdown. A-H. Blood-feeding behaviour of virgin females injected with dsRNA against *Eiger* (A), *Juvenile hormone epoxide hydrolase-1 like (JHEH)* (B), *Orcokinin peptides type-A like (Ork)* (C), *Hairy* (D), *Prothoracicostatic peptides (Prp)* (E), *Na-dependent amino acid transporter-1 like 118504075* (F), *Na-dependent amino acid transporter-1 like 118504077* (G), *118504075+118504077* (H). *dsGFP* was injected as a control in each case. No change in the behavior was observed for any of the candidates tested. 18-25 females/replicate, n=2-6 replicates/group. Unpaired t-test, p<0.05. n.s. not significant, *p<0.05 (A, D, F-H). A'-H'. Relative mRNA expression in the heads of virgin *An. stephensi* females injected with the indicated dsRNA, as compared to that in *dsGFP* injected females, analysed via qPCR. Efficient knockdown could not be achieved for *Hairy* and *Prp.* Unpaired t-test, p<0.05. ****p<0.0001 (A', D'). One way ANOVA with Holm-Šídák multiple comparisons test, p<0.05 (F'-H').

Supplementary Figure S9

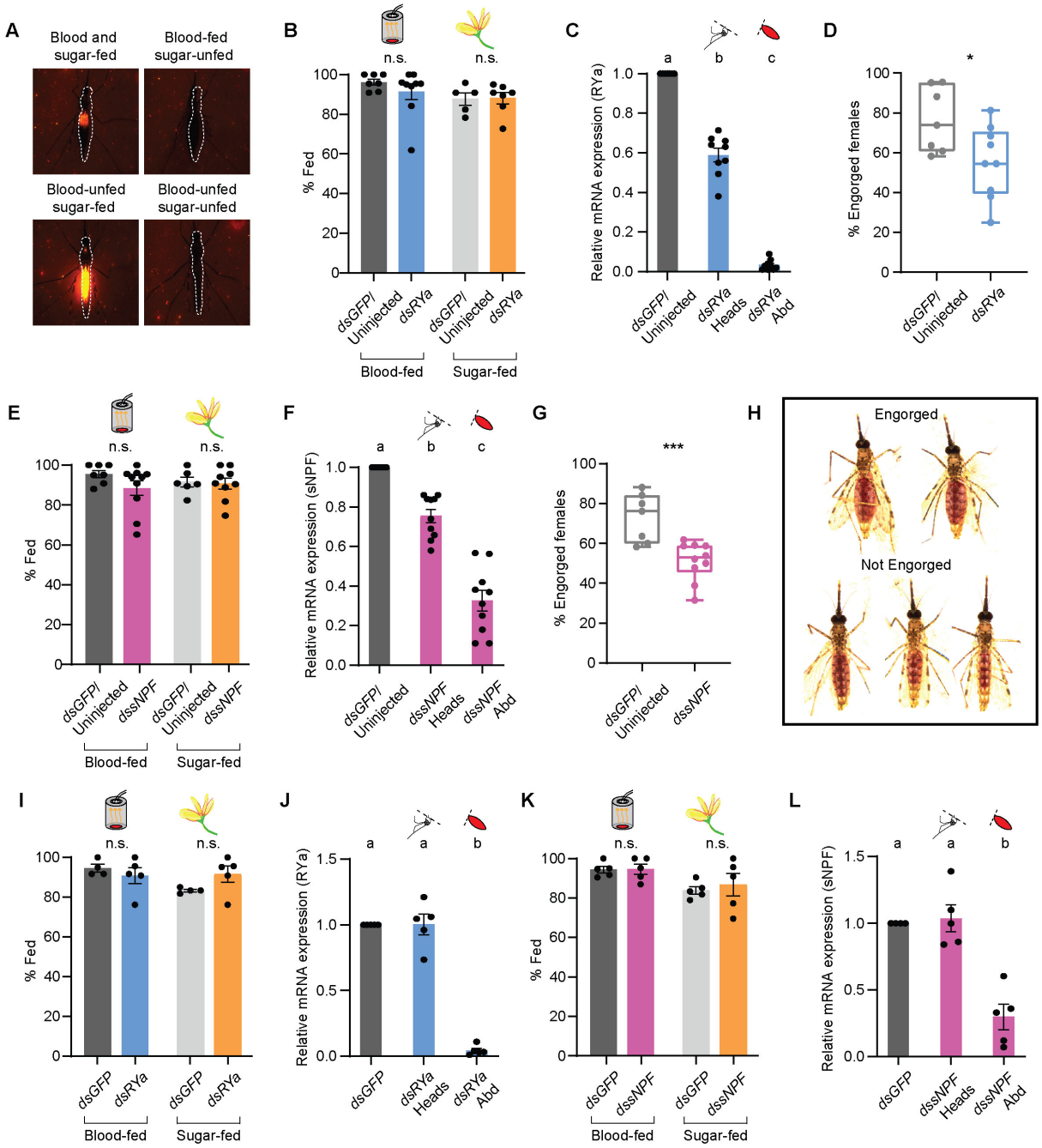

Supplementary Figure 9. Abdominal knockdown of *RYa* or *sNPF* alone does not contribute to the blood-feeding behaviour in *An. stephensi*. A. Widefield fluorescent images of females assayed for both sugar and blood appetite, post-dsRNA injections. Females were injected as described earlier (see methods for details) and offered Rhodamine B-spiked sugar 24h prior to the assay. Blood-feeding behaviour was tested as described earlier. Representative images of females fed on both blood and sugar, blood only, sugar only or none, are shown. B-H. Blood-feeding and sugar-feeding behaviour of virgin females injected with *dsRYa* (B) and *dssNPF* (E). *dsGFP* injected or uninjected females were used as controls. Relative mRNA expression in the heads and abdomens of the injected females were analysed via qPCR (C, F) to assay for the knockdown efficiency in both tissues. Percent females engorged on blood upon injection with *dsRYa* and *dssNPF*, as compared to control females are shown in D and G respectively. Representative widefield images of females considered to be engorged or not, are shown in H. While the mRNA levels in the abdomens were significantly downregulated, efficient knockdown could not be achieved in the heads. Under these conditions, no change in the blood- or sugar-feeding behaviour was observed for either of the targets. However, fewer females were able to fully engorge on blood in both cases and instead took smaller meals. 16-26 females/replicate, n=5-10 replicates/group. Unpaired t-test, $p<0.05$. n.s. not significant, *$p<0.05$, ***$p<0.001$ (B,D,E,G). One way ANOVA with Holm-Šídák multiple comparisons test, $p<0.05$ (C,F). I-L. Blood-feeding and sugar-feeding behaviour of females when *RYa* and *sNPF* are knocked down only in the abdomen. Virgin females were injected with dsRNA against *RYa* (H) and *sNPF* (J) and assayed for both sugar- and blood-appetite, as described before. *dsGFP* injected females were used as controls. Relative mRNA expression in the heads and abdomens of *RYa* (I) and *sNPF* (K) injected females were analysed via qPCR to assay for the knockdown efficiency in both tissues. No change in the blood- or sugar-feeding behaviour was observed when *RYa* or *sNPF* levels were significantly downregulated in the abdomens without altering the levels in the heads, suggesting that neuronal expression is necessary to promote the blood-feeding behaviour. 19-24 females/replicate, n=4-5 replicates/group. Unpaired t-test, $p<0.05$. n.s. not significant (I, K). One way ANOVA with Holm-Šídák multiple comparisons test, $p<0.05$ (J,L).

Supplementary Figure S10

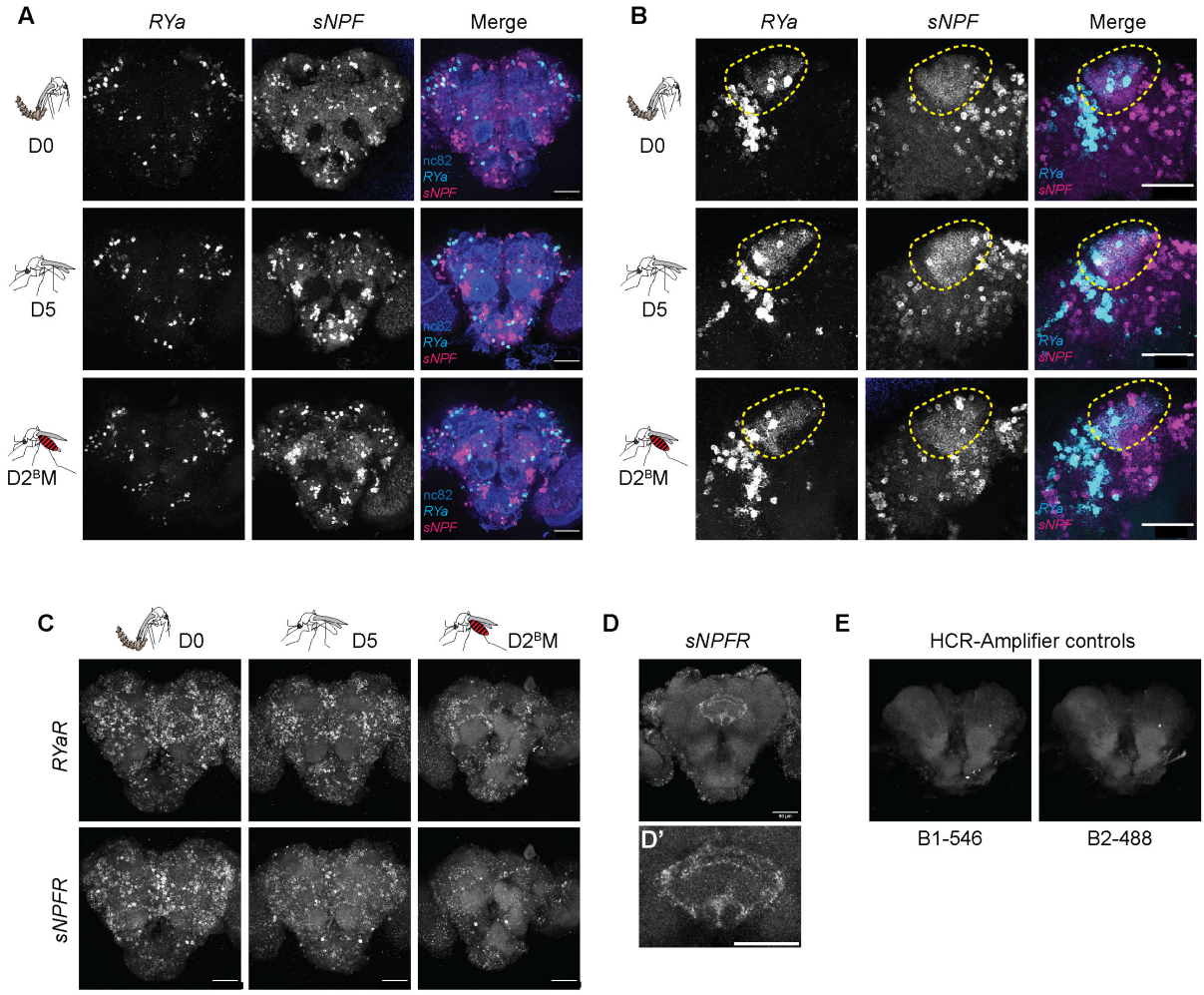

Supplementary Figure 10. Neuropeptides *sNPF*, *RYa* and their receptors are expressed in *An. stephensi* midbrain. A, B. *RYa* and *sNPF* mRNA expression in the midbrains of females uninterested in blood (D0), blood-hungry females (D5) and blood-sated females ($D2^BM$), analysed via HCR. Both neuropeptides are expressed in several clusters across the midbrain (A). While the clusters are largely non-overlapping, co-expression was observed in the Kenyon cells of the mushroom body, indicated by the marked area (B). Maximum intensity projections of confocal stacks are shown. Scale bar, 50µm. C. *RYa receptor (RYaR)* and *sNPF receptor (sNPFR)* mRNA expression in the midbrains of females uninterested in blood (D0), blood-hungry females (D5) and blood-sated ($D2^BM$), analysed via HCR. Both receptors were found to be expressed in multiple cells. Maximum intensity projections of confocal stacks are shown. Scale bar, 50µm. D. *sNPFR* mRNA expression in the central complex. A magnified image is shown in D'. Maximum intensity projection of selected confocal stacks is shown. Scale bar, 50µm. E. Midbrain samples incubated with HCR-Amplifiers only, to serve as a control for background signal in the absence of HCR probes. No signal was observed for either of the amplifiers used (B1 labelled with 546 fluorophore (B1-546) and B2 labelled with 488 fluorophore (B2-488)). (D0: day of emergence; D5: 5days post-emergence, virgin; $D2^BM$: 2days post-blood-meal, mated)

Supplementary Figure S11

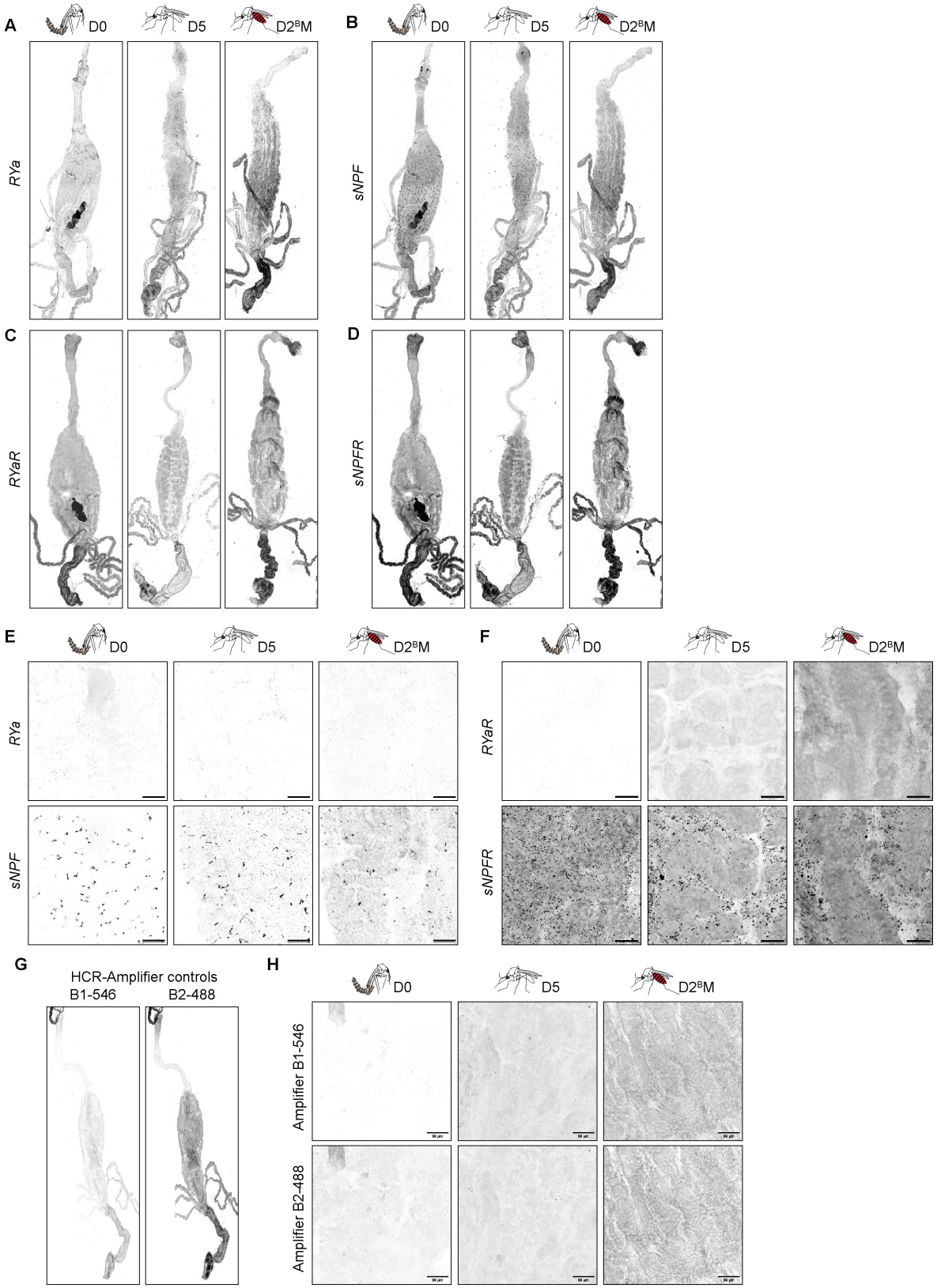

Supplementary Figure 11. *sNPF* and *sNPFR* are expressed in *An. stephensi* posterior midgut. A-F. *RYa* (A), *sNPF* (B), *RYaR* (C) and *sNPFR* (D) mRNA expression in the guts of females uninterested in blood (D0), blood-hungry females (D5) and blood-sated females ($D2^{B}M$), analysed via HCR. Both *sNPF* and its receptor are expressed in the posterior midgut, at all stages analysed. No expression of *RYa* or *RYaR* was observed. Magnified images of the neuropeptides and their receptors are shown in E and F, respectively. Scale bar, 50µm. G,H. Gut samples incubated with HCR-Amplifiers only, to serve as a control for background signal in the absence of HCR probes. No signal was observed for either of the amplifiers used (B1 labelled with 546 fluorophore (B1-546) and B2 labelled with 488 fluorophore (B2-488)).Scale bar, 50µm. (D0: day of emergence; D5: 5days post-emergence, virgin; $D2^{B}M$: 2days post-blood-meal, mated)

Bibliography

1. Verónica María Corrales-Carvajal, Aldo A Faisal, and Carlos Ribeiro. Internal states drive nutrient homeostasis by modulating exploration-exploitation trade-off. *eLife*, 5, oct 2016. ISSN 2050-084X. doi: 10.7554/ELIFE.19920.
2. Md Shahjalal Khan, Redin A Spann, Heike Münzberg, Sangho Yu, Vance L Albaugh, Yanlin He, Hans Rudolf Berthoud, and Christopher D Morrison. Protein Appetite at the Interface between Nutrient Sensing and Physiological Homeostasis. *Nutrients 2021, Vol. 13, Page 4103*, 13(11):4103, 2021. ISSN 2072-6643. doi: 10.3390/NU13114103.
3. Nicholas Heeley and Clemence Blouet. Central amino acid sensing in the control of feeding behavior. *Frontiers in Endocrinology*, 7(NOV):229840, 2016. ISSN 16642392. doi: 10.3389/FENDO.2016.00148/BIBTEX.
4. Gil B Carvalho, Pankaj Kapahi, David J Anderson, and Seymour Benzer. Allocrine Modulation of Feeding Behavior by the Sex Peptide of Drosophila. *Current Biology*, 16(7):692–696, apr 2006. ISSN 0960-9822. doi: 10.1016/j.cub.2006.02.064.
5. Misha A Vargas, Ningguang Luo, Atsushi Yamaguchi, and Pankaj Kapahi. A Role for S6 Kinase and Serotonin in Postmating Dietary Switch and Balance of Nutrients in D. melanogaster. *Current Biology*, 20(11):1006–1011, jun 2010. ISSN 0960-9822. doi: 10.1016/j.cub.2010.04.009.
6. Carlos Ribeiro and Barry J Dickson. Sex peptide receptor and neuronal TOR/S6K signaling modulate nutrient balancing in Drosophila. *Current biology: CB*, 20(11):1000–1005, jun 2010. ISSN 1879-0445. doi: 10.1016/j.cub.2010.03.061.
7. Samuel James Walker, Verónica María Corrales-Carvajal, and Carlos Ribeiro. Postmating Circuitry Modulates Salt Taste Processing to Increase Reproductive Output in Drosophila. *Current biology: CB*, 25(20):2621–2630, oct 2015. ISSN 1879-0445. doi: 10.1016/j.cub.2015.08.043.
8. Meghan Laturney, Gabriella R. Sterne, and Kristin Scott. Mating activates neuroendocrine pathways signaling hunger in Drosophila females. *eLife*, 12, 2023. ISSN 2050084X. doi: 10.7554/ELIFE.85117.
9. Hidehiko K Inagaki, Shlomo Ben-Tabou De-Leon, Allan M Wong, Smitha Jagadish, Hiroshi Ishimoto, Gilad Barnea, Toshihiro Kitamoto, Richard Axel, and David J Anderson. Visualizing neuromodulation in vivo: TANGO-mapping of dopamine signaling reveals appetite control of sugar sensing. *Cell*, 148(3):583–595, 2012. ISSN 1097-4172. doi: 10.1016/J.CELL.2011.12.022.
10. Hidehiko K Inagaki, Ketaki M Panse, and David J Anderson. Independent, reciprocal neuromodulatory control of sweet and bitter taste sensitivity during starvation in Drosophila. *Neuron*, 84(4):806–820, 2014. ISSN 1097-4199. doi: 10.1016/J.NEURON.2014.09.032.
11. Sunanda Marella, Kevin Mann, and Kristin Scott. Dopaminergic Modulation of Sucrose Acceptance Behavior in Drosophila. *Neuron*, 73(5):941–950, 2012. ISSN 0896-6273. doi: 10.1016/J.NEURON.2011.12.032.
12. Anita V Devineni and Kristin M Scaplen. Neural Circuits Underlying Behavioral Flexibility: Insights From Drosophila. *Frontiers in Behavioral Neuroscience*, 15, 2022. ISSN 16625153. doi: 10.3389/FNBEH.2021.821680.
13. Naoko Toshima and Teiichi Tanimura. Taste preference for amino acids is dependent on internal nutritional state in Drosophila melanogaster. *The Journal of experimental biology*, 215(Pt 16):2827–2832, 2012. ISSN 1477-9145. doi: 10.1242/JEB.069146.
14. Anindya Ganguly, Manali Dey, Christi Scott, Vi Khoi Duong, and Anupama Arun Dahanukar. Dietary Macronutrient Imbalances Lead to Compensatory Changes in Peripheral Taste via Independent Signaling Pathways. *The Journal of neuroscience : the official journal of the Society for Neuroscience*, 41(50):10222–10246, 2021. ISSN 1529-2401. doi: 10.1523/JNEUROSCI.2154-20.2021.
15. Molly A Matty, Hiu E Lau, Jessica A Haley, Anupama Singh, Ahana Chakraborty, Karina Kono, Kirthi C Reddy, Malene Hansen, and Sreekanth H Chalasani. Intestine-to-neuronal signaling alters risk-taking behaviors in food-deprived Caenorhabditis elegans. *PLOS Genetics*, 18(5):e1010178, 2022. ISSN 1553-7404. doi: 10.1371/JOURNAL.PGEN.1010178.
16. Michael J Waterson and Tamas L Horvath. Neuronal Regulation of Energy Homeostasis: Beyond the Hypothalamus and Feeding. *Cell Metabolism*, 22(6):962–970, 2015. ISSN 1550-4131. doi: 10.1016/J.CMET.2015.09.026.
17. Emily E LeDue, Kevin Mann, Ellen Koch, Bonnie Chu, Roslyn Dakin, and Michael D Gordon. Starvation-Induced Depotentiation of Bitter Taste in Drosophila. *Current biology : CB*, 26 (21):2854–2861, 2016. ISSN 1879-0445. doi: 10.1016/J.CUB.2016.08.028.
18. Kang I Ko, Cory M Root, Scott A Lindsay, Orel A Zaninovich, Andrew K Shepherd, Steven A Wasserman, Susy M Kim, and Jing W Wang. Starvation promotes concerted modulation of appetitive olfactory behavior via parallel neuromodulatory circuits. *eLife*, 4, 2015. ISSN 2050-084X. doi: 10.7554/ELIFE.08298.
19. Cory M Root, Kang I Ko, Amir Jafari, and Jing W Wang. Presynaptic facilitation by neuropeptide signaling mediates odor-driven food search. *Cell*, 145(1):133–144, 2011. ISSN 1097-4172. doi: 10.1016/J.CELL.2011.02.008.
20. Nao Horio and Stephen D. Liberles. Hunger enhances food-odour attraction through a neuropeptide Y spotlight. *Nature 2021 592:7853*, 592(7853):262–266, mar 2021. ISSN 1476-4687. doi: 10.1038/s41586-021-03299-4.
21. Yiming Chen, Yen Chu Lin, Tzu Wei Kuo, and Zachary A. Knight. Sensory Detection of Food Rapidly Modulates Arcuate Feeding Circuits. *Cell*, 160(5):829–841, feb 2015. ISSN 0092-8674. doi: 10.1016/J.CELL.2015.01.033.
22. Ou Fu, Yuu Iwai, Masataka Narukawa, Ayako W. Ishikawa, Kentaro K. Ishii, Ken Murata, Yumiko Yoshimura, Kazushige Touhara, Takumi Misaka, Yasuhiko Minokoshi, and Ken ichiro Nakajima. Hypothalamic neuronal circuits regulating hunger-induced taste modification. *Nature Communications 2019 10:1*, 10(1):1–14, oct 2019. ISSN 2041-1723. doi: 10.1038/s41467-019-12478-x.
23. Mark L Andermann and Bradford B Lowell. Toward a Wiring Diagram Understanding of Appetite Control. *Neuron*, 95(4):757–778, 2017. ISSN 1097-4199. doi: 10.1016/J.NEURON.2017.06.014.
24. Ryan W S Wee, Karyna Mishchanchuk, Rawan AlSubaie, Timothy W Church, Matthew G Gold, and Andrew F MacAskill. Internal-state-dependent control of feeding behavior via hippocampal ghrelin signaling. *Neuron*, 112(2):288–305.e7, 2024. ISSN 0896-6273. doi: 10.1016/J.NEURON.2023.10.016.
25. Philip K. Shiu, Gabriella R. Sterne, Stefanie Engert, Barry J. Dickson, and Kristin Scott. Taste quality and hunger interactions in a feeding sensorimotor circuit. *eLife*, 11, jul 2022. ISSN 2050-084X. doi: 10.7554/ELIFE.79887.
26. Sercan Sayin, Jean Francois De Backer, K P Siju, Marina E Wosniack, Laurence P Lewis, Lisa Marie Frisch, Benedikt Gansen, Philipp Schlegel, Amelia Edmondson-Stait, Nadiya Sharifi, Corey B Fisher, Steven A Calle-Schuler, J Scott Lauritzen, Davi D Bock, Marta Costa, Gregory S X E Jefferis, Julijana Gjorgjieva, and Ilona C Grunwald Kadow. A Neural Circuit Arbitrates between Persistence and Withdrawal in Hungry Drosophila. *Neuron*, 104 (3):544–558.e6, 2019. ISSN 0896-6273. doi: 10.1016/J.NEURON.2019.07.028.
27. Chang Hui Tsao, Chien Chun Chen, Chen Han Lin, Hao Yu Yang, and Suewei Lin. Drosophila mushroom bodies integrate hunger and satiety signals to control innate food-seeking behavior. *eLife*, 7, 2018. ISSN 2050-084X. doi: 10.7554/ELIFE.35264.
28. Preeti F. Sareen, Li Yan McCurdy, and Michael N. Nitabach. A neuronal ensemble encoding adaptive choice during sensory conflict in Drosophila. *Nature communications*, 12(1), dec 2021. ISSN 2041-1723. doi: 10.1038/S41467-021-24423-Y.
29. Jin Yong Park, Monica Dus, Seonil Kim, Farhan Abu, Makoto I Kanai, Bernardo Rudy, and Greg S B Suh. Drosophila SLC5A11 Mediates Hunger by Regulating K(+) Channel Activity. *Current biology : CB*, 26(15):1965–1974, 2016. ISSN 1879-0445. doi: 10.1016/J.CUB.2016.05.076.
30. Pierre Yves Musso, Pierre Junca, and Michael D. Gordon. A neural circuit linking two sugar sensors regulates satiety-dependent fructose drive in Drosophila. *Science Advances*, 7(49): 186, dec 2021. ISSN 23752548. doi: 10.1126/SCIADV.ABJ0186/SUPPL_FILE/SCIADV.ABJ0186_MOVIES_S1_AND_S2.ZIP.
31. Dennis Goldschmidt, Ibrahim Tastekin, Daniel Münch, Jin-Yong Park, Hannah Haberkern, Lúcia Serra, Célia Baltazar, Vivek Jayaraman, Gerald M. Rubin, and Carlos Ribeiro. A neuronal substrate for translating nutrient state and resource density estimations into foraging decisions. *bioRxiv*, page 2023.07.19.549514, jul 2023. doi: 10.1101/2023.07.19.549514.
32. Qili Liu, Masashi Tabuchi, Sha Liu, Lay Kodama, Wakako Horiuchi, Jay Daniels, Lucinda Chiu, Daniel Baldoni, and Mark N. Wu. Branch-specific plasticity of a bifunctional dopamine circuit encodes protein hunger. *Science*, 356(6337):534–539, may 2017. ISSN 10959203. doi: 10.1126/SCIENCE.AAL3245/SUPPL_FILE/AAL3245_LIU_SM.PDF.
33. Daniel Münch, Dennis Goldschmidt, and Carlos Ribeiro. The neuronal logic of how internal states control food choice. *Nature 2022 607:7920*, 607(7920):747–755, jul 2022. ISSN 1476-4687. doi: 10.1038/s41586-022-04909-5.
34. Jessica Dittmer, Ayad Alafndi, and Paolo Gabrieli. Fat body-specific vitellogenin expression regulates host-seeking behaviour in the mosquito Aedes albopictus. *PLoS biology*, 17(5), 2019. ISSN 1545-7885. doi: 10.1371/JOURNAL.PBIO.3000238.
35. Jeff Liesch, Lindsay L Bellani, and Leslie B Vosshall. Functional and {Genetic} {Characterization} of {Neuropeptide} {Y}-{Like} {Receptors} in {Aedes} aegypti. *PLOS Neglected Tropical Diseases*, 7(10):e2486, 2013. ISSN 1935-2735. doi: 10.1371/journal.pntd.0002486.
36. Peter Christ, Anna Reifenrath, Jörg Kahnt, Frank Hauser, Sharon Rose Hill, Joachim Schachtner, and Rickard Ignell. Feeding-induced changes in allatostatin-a and short neuropeptide f in the antennal lobes affect odor-mediated host seeking in the yellow fever mosquito, aedes aegypti. *PLOS ONE*, 12:e0188243, 11 2017. ISSN 1932-6203. doi: 10.1371/JOURNAL.PONE.0188243.
37. Emely V. Zeledon, Leigh A. Baxt, Tanweer A. Khan, Mayako Michino, Michael Miller, David J. Huggins, Caroline S. Jiang, Leslie B. Vosshall, and Laura B. Duvall. Next Generation Neuropeptide Y Receptor Small Molecule Agonists Inhibit Mosquito Biting Behavior. *bioRxiv*, page 2024.02.28.582529, mar 2024. doi: 10.1101/2024.02.28.582529.
38. Xiaoyi Dou, Kangkang Chen, Mark R. Brown, and Michael R. Strand. Reciprocal interactions between neuropeptide f and ryamide regulate host attraction in the mosquito aedes aegypti. *Proceedings of the National Academy of Sciences of the United States of America*, 121:e2408072121, 7 2024. ISSN 10916490. doi: 10.1073/PNAS.2408072121/SUPPL_FILE/PNAS.2408072121.SAPP.PDF.
39. Laura B Duvall, Lavoisier Ramos-Espiritu, Kyrollos E Barsoum, J Fraser Glickman, and Leslie B Vosshall. Small-Molecule Agonists of Ae. aegypti Neuropeptide Y Receptor Block Mosquito Biting. *Cell*, 176(4):687–701.e5, 2019. ISSN 1097-4172. doi: 10.1016/J.CELL.2018.12.004.
40. Rachel Galun, Y. Avi-Dor, and M. Bar-Zeev. Feeding response in aedes aegypti: Stimulation by adenosine triphosphate. *Science*, 142:1674–1675, 12 1963. ISSN 00368075. doi: 10.1126/SCIENCE.142.3600.1674.
41. Chisako Sakuma, Takeo Iwamoto, Keiko Masuda, Yoshihiro Shimizu, Fumiaki Obata, and Hirotaka Kanuka. Fibrinopeptide a-induced blood-feeding arrest in the yellow fever mosquito aedes aegypti. *Cell Reports*, 43:114354, 7 2024. ISSN 2211-1247. doi: 10.1016/J.CELREP.2024.114354.
42. M. E. Sinka, S. Pironon, N. C. Massey, J. Longbottom, J. Hemingway, C. L. Moyes, and K. J. Willis. A new malaria vector in africa: Predicting the expansion range of anopheles stephensi and identifying the urban populations at risk. *Proceedings of the National Academy of Sciences of the United States of America*, 117:24900–24908, 10 2020. ISSN 1091-6490. doi: 10.1073/PNAS.2003976117.
43. Krithika Venkataraman, Nadav Shai, Priyanka Lakhiani, Sarah Zylka, Jieqing Zhao, Margaret Herre, Joshua Zeng, Lauren A. Neal, Henrik Molina, Li Zhao, and Leslie B. Vosshall. Two novel, tightly linked, and rapidly evolving genes underlie aedes aegypti mosquito reproductive resilience during drought. *eLife*, 12, 2 2023. ISSN 2050084X. doi: 10.7554/ELIFE.80489.
44. Susan M. Villarreal, Sylvie Pitcher, Michelle E.H. Helinski, Lynn Johnson, Mariana F. Wolfner, and Laura C. Harrington. Male contributions during mating increase female survival in the disease vector mosquito aedes aegypti. *Journal of Insect Physiology*, 108:1–9, 7 2018. ISSN 0022-1910. doi: 10.1016/J.JINSPHYS.2018.05.001.
45. Vimla Adlakha and M. K.K. Pillai. Rôle of male accessory gland substance in the regulation of blood intake by mosquitoes. *Journal of Insect Physiology*, 22:1441–1442, 1 1976. ISSN 0022-1910. doi: 10.1016/0022-1910(76)90206-7.
46. Laura B Duvall, Nipun S Basrur, Henrik Molina, Conor J McMeniman, and Leslie B Vosshall. A Peptide Signaling System that Rapidly Enforces Paternity in the Aedes aegypti Mosquito. *Current biology : CB*, 27(23):3734—-3742.e5, dec 2017. ISSN 0960-9822. doi: 10.1016/j.cub.2017.10.074.

47. A J Grant and R J O'Connell. Electrophysiological responses from receptor neurons in mosquito maxillary palp sensilla. *Ciba Foundation Symposium*, 200:233–253,281–284, 1996. ISSN 0300-5208. doi: 10.1002/9780470514948.ch17.
48. Edward E Davis. Development of lactic acid-receptor sensitivity and host-seeking behaviour in newly emerged female Aedes aegypti mosquitoes. *Journal of Insect Physiology*, 30(3): 211–215, jan 1984. ISSN 0022-1910. doi: 10.1016/0022-1910(84)90005-2.
49. A B Omondi, M Ghaninia, M Dawit, T Svensson, and R Ignell. Age-dependent regulation of host seeking in Anopheles coluzzii. *Scientific Reports*, 9(1):9699, jul 2019. ISSN 2045-2322. doi: 10.1038/s41598-019-46220-w.
50. F. T. Takahashi, E. E. Davis, M. Kloza, and Wroclaw Poland Wydawnictwo Politechniki Wroclawskiej. Humoral alteration of chemoreceptor sensitivity in Aedes aegypti following a blood meal Mosquito, host seeking and biting behavior. 1981.
51. Edward E. Davis. Regulation of sensitivity in the peripheral chemoreceptor systems for host-seeking behaviour by a haemolymph-borne factor in Aedes aegypti. *Journal of Insect Physiology*, 30(2):179–183, 1984. ISSN 00221910. doi: 10.1016/0022-1910(84)90124-0.
52. W Takken, null van Loon JJ, and W Adam. Inhibition of host-seeking response and olfactory responsiveness in Anopheles gambiae following blood feeding. *Journal of Insect Physiology*, 47(3):303–310, mar 2001. ISSN 1879-1611. doi: 10.1016/s0022-1910(00)00107-4.
53. Mahul Chakraborty, Arunachalam Ramaiah, Adriana Adolfi, Paige Halas, Bhagyashree Kaduskar, Luna Thanh Ngo, Suvratha Jayaprasad, Kiran Paul, Saurabh Whadgar, Subhashini Srinivasan, Suresh Subramani, Ethan Bier, Anthony A. James, and J. J. Emerson. Hidden genomic features of an invasive malaria vector, Anopheles stephensi, revealed by a chromosome-level genome assembly. *BMC biology*, 19(1), dec 2021. ISSN 1741-7007. doi: 10.1186/S12915-021-00963-Z.
54. Eileen Krüger, Wilson Mena, Eleanor C Lahr, Erik C Johnson, and John Ewer. Genetic analysis of Eclosion hormone action during Drosophila larval ecdysis. *Development (Cambridge)*, 142(24):4279–4287, 2015. ISSN 14779129. doi: 10.1242/DEV.126995/256923/AM/GENETIC-ANALYSIS-OF-ECLOSION-HORMONE-ACTION-DURING.
55. Ching Wei Luo, Elizabeth M. Dewey, Satoko Sudo, John Ewer, Sheau Yu Hsu, Hans Willi Honegger, and Aaron J.W. Hsueh. Bursicon, the insect cuticle-hardening hormone, is a heterodimeric cystine knot protein that activates g protein-coupled receptor lgr2. *Proceedings of the National Academy of Sciences of the United States of America*, 102:2820–2825, 2 2005. ISSN 00278424. doi: 10.1073/PNAS.0409916102/SUPPL_FILE/09916FIG6.JPG.
56. Andrew Brantley Hall, Yumin Qi, Vladimir Timoshevskiy, Maria V Sharakhova, Igor V Sharakhov, and Zhijian Tu. Six novel Y chromosome genes in Anopheles mosquitoes discovered by independently sequencing males and females. *BMC Genomics*, 14(1):1–13, 2013. ISSN 14712164. doi: 10.1186/1471-2164-14-273/TABLES/5.
57. Geoffrey M. Attardo, Immo A. Hansen, and Alexander S. Raikhel. Nutritional regulation of vitellogenesis in mosquitoes: Implications for anautogeny. *Insect Biochemistry and Molecular Biology*, 35(7):661–675, jul 2005. ISSN 0965-1748. doi: 10.1016/J.IBMB.2005.02.013.
58. Zita Carvalho-Santos, Rita Cardoso-Figueiredo, Ana Paula Elias, Ibrahim Tastekin, Célia Baltazar, and Carlos Ribeiro. Cellular metabolic reprogramming controls sugar appetite in Drosophila. *Nature Metabolism 2020 2:9*, 2(9):958–973, aug 2020. ISSN 2522-5812. doi: 10.1038/s42255-020-0266-x.
59. Harinder S Hundal and Peter M Taylor. Amino acid transceptors: gate keepers of nutrient exchange and regulators of nutrient signaling. *American Journal of Physiology - Endocrinology and Metabolism*, 296(4):E603, 2009. ISSN 01931849. doi: 10.1152/AJPENDO.91002.2008.
60. Neha Agrawal, Renald Delanoue, Alessandra Mauri, Davide Basco, Matthieu Pasco, Bernard Thorens, and Pierre Léopold. The Drosophila TNF Eiger Is an Adipokine that Acts on Insulin-Producing Cells to Mediate Nutrient Response. *Cell Metabolism*, 23(4):675–684, 2016. ISSN 19327420. doi: 10.1016/j.cmet.2016.03.003.
61. Tusar T Saha, Sang Woon Shin, Wei Dou, Sourav Roy, Bo Zhao, Yuan Hou, Xue Li Wang, Zhen Zou, Thomas Girke, and Alexander S Raikhel. Hairy and Groucho mediate the action of juvenile hormone receptor Methoprene-tolerant in gene repression. *Proceedings of the National Academy of Sciences of the United States of America*, 113(6):E735–E743, 2016. ISSN 10916490. doi: 10.1073/PNAS.1523838113/-/DCSUPPLEMENTAL.
62. Marla R. Share and R. Michael Roe. A partition assay for the simultaneous determination of insect juvenile hormone esterase and epoxide hydrolase activity. *Analytical Biochemistry*, 169(1):81–88, feb 1988. ISSN 0003-2697. doi: 10.1016/0003-2697(88)90257-6.
63. Dick R. Nässel and Meet Zandawala. Hormonal axes in drosophila: regulation of hormone release and multiplicity of actions. *Cell and Tissue Research*, 382:233, 11 2020. ISSN 14320878. doi: 10.1007/S00441-020-03264-Z.
64. Alina Malita, Olga Kubrak, Takashi Koyama, Nadja Ahrentløv, Michael J. Texada, Stanislav Nagy, Kenneth V. Halberg, and Kim Rewitz. A gut-derived hormone suppresses sugar appetite and regulates food choice in drosophila. *Nature Metabolism 2022 4:11*, 4:1532–1550, 11 2022. ISSN 2522-5812. doi: 10.1038/s42255-022-00672-z.
65. Harry M T Choi, Victor A Beck, and Niles A Pierce. Next-generation in situ hybridization chain reaction: Higher gain, lower cost, greater durability. *ACS Nano*, 8(5):4284–4294, 2014. ISSN 1936086X. doi: 10.1021/NN405717P/SUPPL_FILE/NN405717P_SI_002.AVI.
66. Harry M.T. Choi, Maayan Schwarzkopf, Mark E. Fornace, Aneesh Acharya, Georgios Artavanis, Johannes Stegmaier, Alexandre Cunha, and Niles A. Pierce. Third-generation in situ hybridization chain reaction: multiplexed, quantitative, sensitive, versatile, robust. *Development (Cambridge, England)*, 145(12), jun 2018. ISSN 1477-9129. doi: 10.1242/DEV.165753.
67. Dick R Nässel, Lina E Enell, Jonathan G Santos, Christian Wegener, and Helena A D Johard. A large population of diverse neurons in the Drosophila central nervous system expresses short neuropeptide F, suggesting multiple distributed peptide functions. *BMC Neuroscience*, 9:90, sep 2008. ISSN 14712202. doi: 10.1186/1471-2202-9-90.
68. Ladislav Roller, Daniel Čižmár, Branislav Bednár, and Dušan Žitňan. Expression of RYamide in the nervous and endocrine system of Bombyx mori. *Peptides*, 80:72–79, jun 2016. ISSN 0196-9781. doi: 10.1016/J.PEPTIDES.2016.02.003.
69. Jan A. Veenstra and Hela Khammassi. Rudimentary expression of RYamide in Drosophila melanogaster relative to other Drosophila species points to a functional decline of this neuropeptide gene. *Insect Biochemistry and Molecular Biology*, 83:68–79, apr 2017. ISSN 0965-1748. doi: 10.1016/J.IBMB.2017.03.001.
70. Fei Wang, Kaiyu Wang, Nora Forknall, Christopher Patrick, Tansy Yang, Ruchi Parekh, Davi Bock, and Barry J Dickson. Neural circuitry linking mating and egg laying in Drosophila females. *Nature*, 579(7797):101–105, mar 2020. ISSN 1476-4687. doi: 10.1038/s41586-020-2055-9.
71. Kaiyu Wang, Fei Wang, Nora Forknall, Tansy Yang, Christopher Patrick, Ruchi Parekh, and Barry J Dickson. Neural circuit mechanisms of sexual receptivity in Drosophila females. *Nature*, 589(7843):577–581, jan 2021. ISSN 1476-4687. doi: 10.1038/s41586-020-2972-7.
72. I Alexandra Amaro, Margot P Wohl, Sylvie Pitcher, Catalina Alfonso-Parra, Frank W Avila, Andrew S Paige, Michelle E H Helinski, Laura B Duvall, Laura C Harrington, Mariana F Wolfner, and Conor J McMeniman. Sex peptide receptor is not required for refractoriness to remating or induction of egg laying in Aedes aegypti. *Genetics*, 227(1), mar 2024. ISSN 1943-2631. doi: 10.1093/GENETICS/IYAE034.
73. Jiajia Zhao, Jiaming Yin, Zeng Wang, Jie Shen, Min Dong, and Shuo Yan. Complicated gene network for regulating feeding behavior: novel efficient target for pest management. *Pest management science*, 81, 1 2025. ISSN 1526-4998. doi: 10.1002/PS.8459.
74. Conor J. McMeniman, Román A. Corfas, Benjamin J. Matthews, Scott A. Ritchie, and Leslie B. Vosshall. Multimodal Integration of Carbon Dioxide and Other Sensory Cues Drives Mosquito Attraction to Humans. *Cell*, 156(5):1060, feb 2014. ISSN 10974172. doi: 10.1016/J.CELL.2013.12.044.
75. Gabriella H. Wolff and Jeffrey A. Riffell. Olfaction, experience and neural mechanisms underlying mosquito host preference. *The Journal of experimental biology*, 221(Pt 4), feb 2018. ISSN 1477-9145. doi: 10.1242/JEB.157131.
76. Helena García-Castro, Nathan J. Kenny, Marta Iglesias, Patricia Álvarez-Campos, Vincent Mason, Anamaria Elek, Anna Schönauer, Victoria A. Sleight, Jakke Neiro, Aziz Aboobaker, Jon Permanyer, Manuel Irimia, Arnau Sebé-Pedrós, and Jordi Solana. ACME dissociation: a versatile cell fixation-dissociation method for single-cell transcriptomics. *Genome Biology*, 22(1):1–34, dec 2021. ISSN 1474760X. doi: 10.1186/S13059-021-02302-5/FIGURES/8.
77. Nicolas L. Bray, Harold Pimentel, Páll Melsted, and Lior Pachter. Near-optimal probabilistic RNA-seq quantification. *Nature Biotechnology 2016 34:5*, 34(5):525–527, apr 2016. ISSN 1546-1696. doi: 10.1038/nbt.3519.
78. Sarah E Reese, Kellie J Archer, Terry M Therneau, Elizabeth J Atkinson, Celine M Vachon, Mariza De Andrade, Jean Pierre A Kocher, and Jeanette E Eckel-Passow. A new statistic for identifying batch effects in high-throughput genomic data that uses guided principal component analysis. *Bioinformatics*, 29(22):2877–2883, nov 2013. ISSN 1367-4803. doi: 10.1093/BIOINFORMATICS/BTT480.
79. T S.Keshava Prasad, Ajeet Kumar Mohanty, Manish Kumar, Sreelakshmi K Sreenivasamurthy, Gourav Dey, Raja Sekhar Nirujogi, Sneha M Pinto, Anil K Madugundu, Arun H Patil, Jayshree Advani, Srikanth S Manda, Manoj Kumar Gupta, Sutopa B Dwivedi, Dhanashree S Kelkar, Brantley Hall, Xiaofang Jiang, Ashley Peery, Pavithra Rajagopalan, Soujanya D Yelamanchi, Hitendra S Solanki, Remya Raja, Gajanan J Sathe, Sandip Chavan, Renu Verma, Krishna M Patel, Ankit P Jain, Nazia Syed, Keshava K Datta, Aafaque Ahmed Khan, Manjunath Dammalli, Savita Jayaram, Aneesha Radhakrishnan, Christopher J Mitchell, Chan Hyun Na, Nirbhay Kumar, Photini Sinnis, Igor V Sharakhov, Charles Wang, Harsha Gowda, Zhijian Tu, Ashwani Kumar, and Akhilesh Pandey. Integrating transcriptomic and proteomic data for accurate assembly and annotation of genomes. *Genome Research*, 27(1):133–144, jan 2017. ISSN 15495469. doi: 10.1101/GR.201368.115/-/DC1.
80. Carlos P. Cantalapiedra, Ana Hernandez-Plaza, Ivica Letunic, Peer Bork, and Jaime Huerta-Cepas. eggNOG-mapper v2: Functional Annotation, Orthology Assignments, and Domain Prediction at the Metagenomic Scale. *Molecular Biology and Evolution*, 38(12):5825–5829, dec 2021. ISSN 15371719. doi: 10.1093/MOLBEV/MSAB293.
81. Hedi Peterson, Liis Kolberg, Uku Raudvere, Ivan Kuzmin, and Jaak Vilo. gprofiler2 – an R package for gene list functional enrichment analysis and namespace conversion toolset g:Profiler. *F1000Research*, 9, 2020. ISSN 1759796X. doi: 10.12688/F1000RESEARCH.24956.2.
82. Kenneth J. Livak and Thomas D. Schmittgen. Analysis of relative gene expression data using real-time quantitative pcr and the 2(-delta delta c(t)) method. *Methods (San Diego, Calif.)*, 25:402–408, 2001. ISSN 1046-2023. doi: 10.1006/METH.2001.1262.
83. Heather S Bruce and Gabby Jerz and Sophia not provided Kelly and Jenny not provided McCarthy and Aaron Pomerantz and Gayani Senevirathne and Alice Sherrard and Dennis A Sun and Carsten Wolff and Nipa H Pate. Hybridization Chain Reaction (HCR) In Situ Protocol.
84. Maija Slaidina, Torsten U. Banisch, Selena Gupta, and Ruth Lehmann. A single-cell atlas of the developing drosophila ovary identifies follicle stem cell progenitors. *Genes and Development*, 34:239–249, 2 2020. ISSN 15495477. doi: 10.1101/GAD.330464.119/-/DC1.
85. Johannes Schindelin, Ignacio Arganda-Carreras, Erwin Frise, Verena Kaynig, Mark Longair, Tobias Pietzsch, Stephan Preibisch, Curtis Rueden, Stephan Saalfeld, Benjamin Schmid, Jean Yves Tinevez, Daniel James White, Volker Hartenstein, Kevin Eliceiri, Pavel Tomancak, and Albert Cardona. Fiji: an open-source platform for biological-image analysis. *Nature Methods 2012 9:7*, 9:676–682, 6 2012. ISSN 1548-7105. doi: 10.1038/nmeth.2019.